



THE UNIVERSITY *of* EDINBURGH

Edinburgh Research Explorer

## Age and geochemistry of the Charlestown Group, Ireland

**Citation for published version:**

Herrington, RJ, Hollis, SP, Cooper, MR, Stobbs, I, Tapster, S, Rushton, A, McConnell, B & Jeffries, T 2018, 'Age and geochemistry of the Charlestown Group, Ireland: Implications for the Grampian orogeny, its mineral potential and the Ordovician timescale', *Lithos*, vol. 302-303, pp. 1-19.  
<https://doi.org/10.1016/j.lithos.2017.12.012>

**Digital Object Identifier (DOI):**

[10.1016/j.lithos.2017.12.012](https://doi.org/10.1016/j.lithos.2017.12.012)

**Link:**

[Link to publication record in Edinburgh Research Explorer](#)

**Document Version:**

Peer reviewed version

**Published In:**

Lithos

**General rights**

Copyright for the publications made accessible via the Edinburgh Research Explorer is retained by the author(s) and / or other copyright owners and it is a condition of accessing these publications that users recognise and abide by the legal requirements associated with these rights.

**Take down policy**

The University of Edinburgh has made every reasonable effort to ensure that Edinburgh Research Explorer content complies with UK legislation. If you believe that the public display of this file breaches copyright please contact [openaccess@ed.ac.uk](mailto:openaccess@ed.ac.uk) providing details, and we will remove access to the work immediately and investigate your claim.



1 Age and geochemistry of the Charlestown Group, Ireland: implications  
2 for the Grampian orogeny, its mineral potential and the Ordovician  
3 timescale

4  
5 Richard J. Herrington<sup>1\*</sup>, Steven P. Hollis<sup>2,3</sup>, Mark R. Cooper<sup>4</sup>, Iain Stobbs<sup>5,6</sup>,  
6 Simon Tapster<sup>7</sup>, Adrian Rushton<sup>8</sup>, Brian McConnell<sup>3</sup> & Teresa Jeffries<sup>9</sup>

7  
8 <sup>1</sup>LODE (London Centre for Ore Deposits and Exploration) Department of Earth Sciences,  
9 Natural History Museum, London, SW7 5BD, UK

10 <sup>2</sup>iCRAG (Irish Centre for Research in Applied Geosciences) and School of Earth Sciences,  
11 University College Dublin, Belfield, Dublin 4, Ireland

12 <sup>3</sup>Geological Survey Ireland, Beggars Bush, Haddington Road, Dublin 4, Ireland

13 <sup>4</sup>Geological Survey of Northern Ireland, Dundonald House, Upper Newtownards Road,  
14 Belfast, BT4 3SB, UK

15 <sup>5</sup>Imperial College, Exhibition Road, London, SW7 2AZ, UK

16 <sup>6</sup>School of Ocean and Earth Science, National Oceanography Centre, European Way,  
17 Southampton University, Southampton, SO14 3ZH, UK.

18 <sup>7</sup>NERC Isotope Geosciences Laboratory, British Geological Survey, Keyworth, Nottingham,  
19 NG12 5GG, UK.

20 <sup>8</sup>Department of Earth Sciences, Natural History Museum, London, SW7 5BD, UK

21 <sup>9</sup>Core Research Laboratories, The Natural History Museum, London SW7 5BD, UK

22

23 To submit to: *Lithos*

24

25 Keywords: Grampian, Taconic, graptolite, biostratigraphy, U-Pb zircon, Caledonian,  
26 Appalachian, VMS, timescale (calibration)

27

28 \*Corresponding author: [r.herrington@nhm.ac.uk](mailto:r.herrington@nhm.ac.uk)

29

30 **ABSTRACT**

31 Accurately reconstructing the growth of continental margins during episodes of ocean closure  
32 has important implications for understanding the formation, preservation and location of  
33 mineral deposits in ancient orogens. The Charlestown Group of county Mayo, Ireland, forms  
34 an important yet understudied link in the Caledonian-Appalachian orogenic belt located  
35 between the well documented sectors of western Ireland and Northern Ireland. We have  
36 reassessed its role in the Ordovician Grampian orogeny, based on new fieldwork, high-  
37 resolution airborne geophysics, graptolite biostratigraphy, U-Pb zircon dating, whole rock  
38 geochemistry, and an examination of historic drillcore from across the volcanic inlier. The  
39 Charlestown Group can be divided into three formations: Horan, Carracastle, Tawnyinah. The  
40 Horan Formation comprises a mixed sequence of tholeiitic to calc-alkaline basalt, crystal tuff  
41 and sedimentary rocks (e.g. black shale, chert), forming within an evolving peri-Laurentian  
42 affinity island arc. The presence of graptolites *Pseudisograptus* of the *manubriatus* group and  
43 the discovery of *Exigraptus uniformis* and *Skiagraptus gnomonius* favour a latest Dapingian  
44 (i.e. Yapeenian Ya 2 / late Arenig) age for the Horan Formation (equivalent to c. 471.2-470.5  
45 Ma according to the timescale of Sadler et al., 2009). Together with three new U-Pb zircon  
46 ages of 471.95-470.82 Ma from enclosing felsic tuffs and volcanic breccias, this fauna provides  
47 an important new constraint for calibrating the Middle Ordovician timescale. Overlying  
48 deposits of the Carracastle and Tawnyinah formations are dominated by LILE- and LREE-  
49 enriched calc-alkaline andesitic tuffs and flows, coarse volcanic breccias and quartz-feldspar  
50 porphyritic intrusive rocks, overlain by more silicic tuffs and volcanic breccias with rare  
51 occurrences of sedimentary rocks. The relatively young age for the Charlestown Group in the  
52 Grampian orogeny, coupled with high Th/Yb and zircon inheritance (c. 2.7 Ga) in intrusive  
53 rocks indicate the arc was founded upon continental crust (either composite Laurentian margin  
54 or microcontinental block). Regional correlation is best fitted to an association with the post-  
55 subduction flip volcanic/intrusive rocks of the Irish Caledonides, specifically the late-stage  
56 development of the Tyrone Igneous Complex, intrusive rocks of Connemara (western Ireland)  
57 and the Sliswood Division (Co. Sligo). Examination of breccia textures and mineralization  
58 across the volcanic inlier questions the previous porphyry hypothesis for the genesis of the  
59 Charlestown Cu deposit, which are more consistent with a volcanogenic massive sulfide  
60 (VMS) deposit.

61

62

## 63 1. Introduction

64 Accurately reconstructing the growth of continental margins during episodes of ocean closure  
65 has important implications for understanding the formation, preservation and location of  
66 mineral deposits in ancient orogens (van Staal, 2007; Rogers et al., 2007; Herrington and  
67 Brown, 2011; Herrington et al., 2017). Orthomagmatic and volcanogenic massive sulfide  
68 (VMS) deposits may be preserved in accreted oceanic tracts or rifted island arcs (Herrington et  
69 al., 2005; Piercey, 2011), whereas mesothermal gold mineralization typically forms during the  
70 later stages of orogenesis associated with orogenic collapse and deep-seated crustal structures  
71 (Kerrich et al. 2005, Herrington and Brown, 2011). An integrated approach using detailed field  
72 mapping, whole rock geochemistry, U-Pb zircon geochronology and biostratigraphy forms a  
73 powerful tool for unraveling complex orogens, and may highlight the prospectivity of accreted  
74 terranes for different styles of mineralization.

75 The Caledonian-Appalachian orogenic belt records the opening of the Iapetus ocean  
76 during the late Proterozoic (c. 565 Ma: van Staal et al., 2014; **Fig. 1a**) and the events associated  
77 with its closure during the early Paleozoic (Dewey, 2005; Draut et al., 2004; Chew et al., 2010;  
78 Cooper et al., 2013). The Grampian event preserves the first major phase of this closure in the  
79 British and Irish Caledonides, and was associated with the accretion of ophiolites, island arcs  
80 and microcontinental blocks to the Laurentian margin between the Late Cambrian and Middle  
81 Ordovician (Dewey and Shackleton, 1984; Draut et al., 2004; Dewey and Mange, 1999; Cooper  
82 et al., 2011; Chew et al., 2008, 2010; Hollis et al., 2012). The Grampian is broadly equivalent  
83 to the Taconic event of the Canadian Appalachians (van Staal et al., 2007; **Fig. 1b-c**), with  
84 VMS deposits that developed in oceanic and arc/backarc settings (Piercey, 2007) emplaced  
85 during three phases of arc/ophiolite accretion (van Staal et al. 2007; 2014).

86 Figure 2 shows the broad evolution of the Grampian orogeny as it applies to the current  
87 region of study, based on the three equivalent and well-documented arc/ophiolite accretion  
88 events in the Newfoundland Appalachians (modified after van Staal et al. 2007; 2014; Chew  
89 et al. 2010; Hollis et al. 2012). In the British and Irish Caledonides, the accretion of early c.  
90 510-495 Ma suprasubduction affinity oceanic crust (e.g. Deer Park Complex, Highland  
91 Boundary ophiolite, Chew et al., 2010) occurred shortly after its formation, most likely onto  
92 outboard blocks of Laurentian-affinity microcontinental crust (**Fig. 2a**; see Chew et al., 2010).  
93 As ocean closure continued, subduction was associated with the development of the juvenile  
94 c. 490-477 Ma Lough Nafoeey arc system (i.e. Lough Nafoeey Group: Ryan et al., 1980; Draut  
95 et al., 2004; Chew et al. 2007; Ryan and Dewey, 2011; McConnell et al., 2009; **Fig. 1a, Fig.**  
96 **2b**), with its accretion to the Laurentian margin constrained to c. 484-477 Ma (Draut et al.,

97 2004; Hollis et al., 2013a). Syncollisional volcanism during the deposition of the c. 477-468  
98 Tourmakeady Group (**Fig. 2c**) was contemporaneous with Grampian deformation and  
99 metamorphism (c. 475-465 Ma; Friedrich et al., 1999a,b; Chew et al., 2008). Following a  
100 reversal in subduction polarity (from south to northward directed), magmatic activity in  
101 western Ireland is recorded by the eruption of c. 464 Ma ignimbrites of the Murrisk Group  
102 (Dewey and Mange, 1999) and the continued emplacement of granitic rocks across the  
103 Connemara terrane (Friedrich et al. 1999a; **Fig. 1a, Fig. 2d**).

104 The c. 484-470 Ma Tyrone and Ballantrae arc-ophiolite complexes most likely record  
105 the development of an arc system distinct to that of western Ireland (Hollis et al., 2012, 2013ab;  
106 Stone, 2014; **Fig. 1a, Fig. 2b, d**). In the west of Ireland, the Lough Nafoeey arc developed  
107 from c. 490 Ma above a south-dipping subduction zone away from the Laurentian margin (**Fig.**  
108 **2b**), whilst the Tyrone and Ballantrae arcs are much younger, were accreted later (**Fig. 2d**;  
109 Hollis et al., 2013a), and show evidence for widespread arc-rifting and VMS-style  
110 mineralization (Hollis et al., 2014). The accretion of these younger arcs to outboard fragments  
111 of microcontinental crust (such as the Tyrone Central Inlier and Midland Valley block; prior  
112 to c. 470 Ma in Tyrone) was followed by the emplacement of continental arc intrusive rocks  
113 across the composite Laurentian margin until at least c. 464 Ma in Ireland (Cooper and  
114 Mitchell, 2004; Flowerdew et al., 2005; Cooper et al., 2011) and c. 457 in Scotland (Oliver et  
115 al., 2000, 2008; Carty et al., 2013). Remnants of peri-Laurentian affinity island arcs also occur  
116 along the Iapetus Suture zone south of the Southern Uplands – Down-Longford accretionary  
117 prism, such as at Grangegeeth (McConnell et al., 2010) (**Fig. 1a**).

118 The Charlestown Group, exposed across approximately 45 km<sup>2</sup> of Co. Mayo, Ireland  
119 (**Fig. 3**), forms an important link between the well documented Grampian rocks of western  
120 Ireland (Clift and Ryan, 1994; Dewey and Mange, 1999; Draut et al., 2002, 2004) and Northern  
121 Ireland (Hutton et al., 1985; Cooper et al., 2008; Chew et al., 2008; Draut et al., 2009; Cooper  
122 et al., 2011; Hollis et al., 2012). Previous work has largely been restricted to field mapping and  
123 graptolite biostratigraphy (e.g. Cummins, 1954; O'Connor, 1987; Dewey et al., 1970), and  
124 consequently it was not clear whether the Charlestown Group formed during the syncollisional  
125 stage of the Lough Nafoeey arc system (broadly correlating with the Tourmakeady Group; see  
126 review by Chew, 2009), or as part of the younger Tyrone arc system (Hollis et al., 2013a). The  
127 latter is considered prospective for VMS mineralization (Clifford et al., 1992; Peatfield, 2003;  
128 Hollis et al., 2014, 2016) and its accretion to the Laurentian margin has been implicated in  
129 subsequent mesothermal Au mineralization in the overlying Dalradian Supergroup at

130 Curraghinalt (Earls et al., 1996; Parnell et al., 2000; Herrington and Brown, 2011; Rice et al.,  
131 2016).

132 Here we present the results of new fieldwork, whole rock geochemistry, airborne  
133 geophysics from the Tellus Border project, and the first U-Pb zircon ages for the Charlestown  
134 Group. In addition, we have refined biostratigraphic age constraints based on a new graptolite  
135 locality and a reexamination of a fauna collected by Cummins (1954). This work has important  
136 implications for understanding the evolution of the Grampian orogeny and the calibration of  
137 the Middle Ordovician timescale. Implications for base metal mineralization in County Mayo  
138 are discussed based on examination of drillcore from across the volcanic inlier.

139

## 140 **2. Previous work**

141 Although the Charlestown Group forms an integral part of the Irish Caledonides, published and  
142 unpublished research is limited to a handful of studies (Cummins, 1954; Charlesworth, 1960;  
143 Dewey et al., 1970; O'Connor and Poustie, 1986; O'Connor, 1987; Long et al., 2005). The  
144 Charlestown Group is unconformably overlain to the east by Silurian cover sequences, which  
145 together form the Charlestown Inlier, and bounded to the south, north and west by  
146 Carboniferous rocks (**Fig. 3a**). Cummins (1954) originally divided the sequence into an older  
147 tuffaceous group with agglomerates, lavas, fine tuffs interbedded with cherty graptolitic shales;  
148 and the structurally lower felsic group to the south, with subsidiary tuffs and lavas. An Arenig  
149 age was obtained for the lower part of the Charlestown Group (Cummins, 1954), later refined  
150 by Dewey et al. (1970) to the Yapeenian stage of the Australian sequence. Charlesworth (1960)  
151 provided the first detailed structure and stratigraphy of the succession, and based around new  
152 exposure O'Connor (1987 unpublished PhD thesis) reassessed the stratigraphy and divided the  
153 succession into three formations (see **Fig. 3a**), renamed by Long et al. (2005):

154 (i) Horan Formation (lowest unit – formerly known as the Airport Mixed Formation),  
155 ~630 m thick, characterized by minor sedimentary rocks (i.e. red cherts, siltstones and  
156 silicified black shales), extrusive basalts, spillites and mixed tuffs which crop out along  
157 the hinge of the Lurga Anticline. The upper boundary of this formation is defined as  
158 the southern southeast dipping contact of the pyroxene diorite, as shown in **Figure 3a**.  
159 (ii) Carracastle Formation (formerly known as the Carracastle Andesitic Formation),  
160 ~290 m thick, dominated by andesitic tuffs and flows, with coarse volcanic breccias.  
161 The formation is characterized by a general lack of sedimentary rocks, a dominance of  
162 pyroxene-feldspar porphyry over quartz-feldspar porphyry (QFP) derived lithologies,

163 and the presence of thick ungraded volcanic breccias which are almost exclusively  
164 andesitic.

165 (iii) Tawnyinah Formation (formerly known as the Cloonnamna Formation), ~300 m  
166 thick, dominated by more silicic (crystal, ash and lapilli) tuffs and volcanic breccias.  
167 Some sedimentary rocks (black silty tuffs) have been observed in drillcore and rare  
168 occurrences of chert in outcrop. On the southern limb of the Lurga Anticline, the  
169 formation is silicified, chloritized and/or sericitised due to the formation of the  
170 Charlestown Cu deposit.

171 Nowhere are the contacts between the formations currently exposed, the boundary between the  
172 Carracastle and Tawnyinah is defined by O'Connor (1987) as the first occurrence of quartz-  
173 feldspar crystal tuffs and light coloured silicic ashes, an observation presumably based on  
174 drillcore evidence in addition to surface mapping.

175 A detailed account of key exposures and field relationships across the Charlestown  
176 Group are given in O'Connor (1987). O'Connor and Poustie (1986) recorded the presence of  
177 abundant breccia units at Charlestown associated with quartz-feldspar porphyritic rocks, with  
178 mineralization hosted within intrusive units showing sheet-like morphologies. Four breccia  
179 types were described (**Fig. 4**) with their 'type 1' consistent with shallow intrusions of felsic  
180 magmas and unconsolidated mudrocks or tuffs, forming brecciated intrusive rocks injected  
181 with unconsolidated sediment (by definition forming peperites). These breccias are found along  
182 the margins of the quartz-feldspar porphyry units. In one case, chalcopyrite mineralization  
183 directly associated with the development of this peperitic brecciation. In other cases, silicic  
184 alteration appears to be always associated with these high-level porphyry units, whilst the three  
185 other types of breccia relate to autobrecciation or hydraulic fracturing during magma  
186 emplacement (**Fig. 4**).

187 Sub-economic mineralization at Charlestown is developed within and confined to the  
188 hydrothermally altered brecciated sill-like bodies of felsic porphyry. The defined resource is 3  
189 Mt grading 0.6% Cu with subsidiary resources of Zn-Pb-Ba-Ag mineralization (O'Connor and  
190 Poustie, 1986; **Fig. 3a**). The alteration is described as largely comprising concentric zones of  
191 silicic, sericitic, sericitic-chloritic and chloritic, with clay-rich zones associated with sericitic  
192 alteration (**Fig. 4**). Also recorded are poorly constrained zones of hematization. Mineralization  
193 is largely spatially linked to the zones of silicic alteration, but is also described in the sericitic  
194 alteration zone. Chalcopyrite, sphalerite and galena are the dominant minerals of economic  
195 interest, mainly developed in fractures in brecciated silicic-altered rocks. This fracturing type  
196 constitutes O'Connor and Poustie's (op cit.) 'type 4 breccia' which the authors link to processes

197 of hydraulic fracturing. Widespread pyrite represents the earliest phase of sulfide  
198 mineralisation, followed by successively chalcopyrite, sphalerite and barite. Galena with barite  
199 represents the last phase of mineralization.

200 Previous geochemical data from the Charlestown Group are limited to major element data  
201 plus Zr, Rb, Sr, Cu and Zn, with trace elements Ni, Y, Nb, Th, U and Pb frequently near or  
202 below detection levels (O'Connor, 1987). No rare earth element (REE) geochemistry data prior  
203 to our work have been published.

204

205

### 206 **3. Sampling and methods**

207 Major exposures described by O'Connor (1987) were visited during 2012 and 2013, with  
208 additional traverses made across the well exposed Knock Airport section of the pyroxene  
209 diorite and uppermost Horan Formation (**Fig. 3a**, locality C). The stratigraphy through this  
210 sequence (from 146991E 296428N to 146949E 296469N Irish Grid) is described below and  
211 shown in **Figure 5**. Samples were collected from this section and elsewhere for petrography,  
212 whole rock geochemistry (**Fig. 2b**), U-Pb zircon CA-ID-TIMS geochronology, and  
213 biostratigraphy.

214 Of 46 samples collected from the Charlestown Group, 18 were characterized by optical  
215 microscopy and SEM analysis. These included samples from three diamond drillholes through  
216 the Charlestown Group, which were logged to better understand the nature of the hydrothermal  
217 alteration and mineralization across the inlier. Core from these holes (2137-14, 2137-16 and  
218 2137-17: **Fig. 3b**) is stored at the GSI core shed, Dublin, summarized in Section 4, and  
219 described in detail in Stobbs (2013 unpublished MSci thesis).

220

#### 221 **3.1. Tellus Border Geophysics**

222 The Tellus Border project (Hodgson and Ture, 2014) was an as an EU INTERREG IVA-  
223 funded regional mapping project collecting geo-environmental data on soils, water and rocks  
224 across the six border counties of Ireland, continuing the analysis of existing data in Northern  
225 Ireland (Young and Donald, 2013) to produce seamless data coverage over the island of  
226 Ireland. The geophysical survey was completed in 2012 and was flown at 200m line spacing  
227 orientated towards 345°. Magnetic field (**Fig. 3b**), electromagnetic conductivity, and  
228 radiometric (Th, U, K) data were acquired (Hodgson and Ture, 2014). An extension of the  
229 Tellus Border EU project area to cover the adjacent area of the Charlestown Group was co-  
230 funded by Oriel Selection Trust Ltd as part of a mineral exploration programme.



231

### 232 **3.2 Biostratigraphy**

233 Two principal collections of Ordovician fossils have been studied from the Charlestown Inlier.  
234 The first of these was made and reported on by Cummins (1954). Part of this initial collection,  
235 preserved in the Sedgwick Museum, Cambridge, was reexamined. The second collection was  
236 made in 2012 and 2013 by the authors, from a new temporary exposure immediately north of  
237 Knock International Airport (graptolite locality C in **Fig. 3a**) within the upper Horan  
238 Formation. The base of the Horan Formation is not seen at Charlestown. This locality is thought  
239 to lie close to the original site of Cummins (Irish Grid approx. 147900E 295900N, locality A  
240 in **Fig. 3a**), which was not located during recent fieldwork. Locality B of Cummins (1954) has  
241 yielded only fragmentary and indeterminable graptolites.

242

### 243 **3.3 U-Pb Geochronology**

244 Four samples (KGC1-3,5) were selected for LA-ICPMS U-Pb zircon geochronology at the  
245 Natural History Museum, London, to constrain the age of the Horan Formation. Samples were  
246 processed using standard techniques at Trinity College Dublin by Quentin Crowley who  
247 produced heavy mineral separates. Zircon grains were hand-picked and mounted in epoxy  
248 resin. The grains were sectioned and polished. Reflected and transmitted light  
249 photomicrographs and cathodoluminescence (CL) SEM images were prepared for all zircon  
250 grains. The CL images were used to decipher the internal structures of the sectioned grains and  
251 to target specific areas within the zircon crystals.

252 The grains were initially analyzed in the Department of Mineralogy, Natural History  
253 Museum, London, using an ESI New Wave UP193FX laser ablation system coupled to an  
254 Agilent 7500cs quadrupole-based ICP-MS. Samples and standards, mounted together, were  
255 ablated in an air-tight sample chamber flushed with either Ar or He for sample transport. The  
256 samples were rastered up and down lines, using a constant raster speed for each analysis. Data  
257 were collected in discrete runs of 20 analyses, comprising 12 unknowns bracketed before and  
258 after by 4 analyses of the standard zircon 91500 (Wiedenbeck et al., 1995). Data were collected  
259 for up to 180 s per analysis with a gas background taken during the initial ca. 60 s. Background  
260 and mass bias corrected signal intensities and counting statistics were calculated for each  
261 isotope. Concordia age calculations, weighted averages, intercept ages and plotting of  
262 concordia diagrams were performed using Isoplot/Ex rev. 2.49 (Ludwig, 2001). For each  
263 analysis, time resolved signals were collected and then carefully studied to ensure that only flat

264 stable signal intervals were included in the age calculations. The detailed analytical procedure  
265 is outlined in Jeffries et al. (2003). Data are presented as **Supplementary Material**.

266 Following LA-ICPMS screening, zircons were selected and removed from epoxy  
267 mounts for high-precision chemical abrasion isotope dilution thermal ionization mass  
268 spectrometry (CA-ID-TIMS) analysis at the NERC Isotope Geosciences laboratory, British  
269 Geological Survey, Keyworth. The methodology for analytical procedure, instrument  
270 conditions, corrections and data reduction follows that outlined in detail in Tapster et al.,  
271 (2016). The key features for this study are that: (1) zircons removed from the epoxy mounts  
272 were annealed at 900°C for 60 hrs and leached in high-pressure vessels in 29N HF for 10-12  
273 hrs at 180°C as part of the chemical abrasion technique to reduce open system behavior within  
274 the crystals (Mattinson, 2005); (2) Zircons were spiked with the mixed ( $\pm^{202}\text{Pb}$ )– $^{205}\text{Pb}$ – $^{233}\text{U}$ –  
275  $^{235}\text{U}$  EARTHTIME tracer solutions (ET535; ET2535; Condon et al., 2015; Mclean et al., 2015);  
276 (3)  $^{206}\text{Pb}/^{238}\text{U}$  dates were corrected for initial Th disequilibrium with a  $\text{Th}/\text{U}_{(\text{melt})} = 3.5 (\pm 1; 1\sigma)$ .  
277 Uncertainties on the best age interpretations are presented in the form  $\pm x/y/z (2\sigma)$ , where  $x =$   
278 analytical uncertainty only, permitting comparison with data sets using the EARTHTIME  
279 tracers;  $y =$  analytical and tracer calibration uncertainty for comparison with U-Pb data sets  
280 that do not use EARTHTIME tracers;  $z =$  total uncertainty including U decay constants for  
281 comparison with dates yielded by other radio-isotopic systems. Data are presented in **Table 1**.

282

### 283 **3.4 Geochemistry**

284 Fifteen samples from representative units across the Charlestown Group were analyzed for  
285 whole rock geochemistry at the Natural History Museum, London. Samples were collected  
286 from field localities and diamond drillcore. Element concentrations were obtained by fusing  
287 whole rock powders with lithium metaborate flux and subsequent digestion by concentrated  
288 HF, HNO<sub>3</sub> and HClO<sub>4</sub>. This method ensured all zircon and other resistive minerals were  
289 destroyed. Solutions were analyzed by ICP-AES (Thermo iCap 6500 Duo) for major and minor  
290 elements and ICP-MS (Agilent 7700x) for trace element analysis. All samples selected for  
291 geochemical analysis were also characterized by X-Ray Diffraction (XRD) at the Natural  
292 History Museum, London. Additional information is presented in Stobbs (2013), with  
293 geochemical data included as **Supplementary Material**.

294

## 295 **4. Results**

### 296 **4.1. Geology of the Charlestown Group**

297 The geology of the Charlestown Group has been comprehensively described by O'Connor  
298 (1987), as summarized in section 2 above. Here we supplement that account with new  
299 observations from Tellus Border geophysics (**Fig. 3b**), the well exposed Knock Airport section  
300 of the Horan Formation (**Fig. 5**), diamond drillcore, and key outcrops in the Carracastle and  
301 Tawnyinah formations. These results have significant implications for understanding the  
302 genesis of the Charlestown Cu deposit.

303

#### 304 **4.1.1 Tellus Border Geophysics**

305 Due to the generally poor exposure of the Charlestown Group the new Tellus Border  
306 geophysical data provides new insight into the structure of the inlier and its extension beneath  
307 Carboniferous cover sequences (**Fig. 3b**). The Charlestown Group shows a distinctive pattern  
308 in the total magnetic intensity (TMI) data and it can be clearly extrapolated to extend under  
309 Carboniferous cover for at least 4 km to the NE and 10 km to the SW. Only the SE limb of the  
310 mapped Horan Formation appears to be highly magnetic, coincident to where mafic rocks are  
311 well exposed along road cuttings. Significant magnetite was confirmed in samples CT-114 and  
312 12-0339 by XRD. The NE limb of the Horan Formation dominated by crystal tuff and  
313 sedimentary rocks (**Fig. 5**) has a low magnetic signature, as do the Carracastle and Tawnyinah  
314 formations. Drillhole data suggest that several small TMI highs throughout these formations  
315 correspond either to localized occurrences of mafic rocks (e.g. drillhole 2137-14, see  
316 following) or intrusive quartz-feldspar porphyry (QFP) units (such as those SW of drillholes  
317 2137-14 and 2137-17, and near the Charlestown Cu deposit: **Fig. 3b**). Two circular magnetic  
318 features approximately 2 km by 4 km located to the east of the Charlestown Group most likely  
319 represent Late Caledonian intrusions concealed under Carboniferous rocks. These are sited on  
320 the southerly extension of the deep-seated Donegal Lineament. Deep seated crustal lineaments  
321 are well documented across the north of Ireland, influencing Neoproterozoic sedimentation  
322 patterns, and the location of Proterozoic to Late Caledonian magmatism and mineral deposits  
323 (Cooper et al., 2013).

324

#### 325 **4.1.2 Breccia types, hydrothermal alteration and mineralization**

326 The Knock Airport section of the Horan Formation is dominated by banded and stratified tuff  
327 interbedded with finely laminated, silicified black mudstones (**Fig. 5**). Local sills of pyroxene  
328 diorite locally intrude the stratigraphy and it is evident these intrusions are both synvolcanic  
329 and high-level. Intermediate crystal tuffs of the Horan Formation occur where these magmas  
330 were locally erupted.

331 The QFP units throughout the Charlestown stratigraphy most likely represent the high-  
332 level intrusive equivalent of the more silicic tuffs. The development of peperitic textures in the  
333 Charlestown QFP units was observed in a number of places exposed along the Knock Airport  
334 road, confirming the subvolcanic high-level nature of these units and the cause of the type 1  
335 brecciation described by O'Connor and Poustie (1986; **Fig. 4**). The unit observed in the airport  
336 road cutting is largely unmineralized, although fragments of mudrocks rarely contain  
337 disseminated pyrite. The QFP unit shows epidote alteration in a number of places.

338 A felsic crystal tuff unit is exposed in the road cross-section adjacent to an isolated  
339 exposure of a pillowed basaltic unit (**Fig. 3b**). Chloritic alteration and the development of  
340 minor hematite is evident in hand specimen (sample CT113). In thin section, the presence of  
341 hematite and barite was confirmed within chlorite-rutile aggregates forming infilling to  
342 sericite-altered feldspar crystal tuff. SEM analysis indicated highly anomalous copper (>200  
343 ppm) in the Fe-oxide masses (**Fig. 6a**).

344 The autobrecciated QFP intrusives of the Carracastle formation (**Fig. 4**) show distinct  
345 evidence for hydrothermal alteration. In thin section (CT206), abundant irregular voids are  
346 developed between highly altered pyroxene and feldspar phyric fragments with the voids  
347 infilled by cryptocrystalline quartz and barite, suggesting that hydrothermal silica, calcite and  
348 barite infilled the autobreccia (likely type 3 breccia; **Fig. 6b**).

349 Only three drillholes from the sub-surface drilling have been preserved. These three  
350 cores all show evidence for extensive hydrothermal alteration. Drillhole 2137-14 (**Fig. 3b**)  
351 comprises predominantly chert and clastic rocks interbedded with felsic tuffs within the  
352 Carracastle Formation, and is located near to the Knock Airport runway. The unit here is  
353 variably silicified, hematized and chloritized. Samples of volcanic breccia (possibly type 2 or  
354 type 3; 12-0326) and a vesicular mafic volcanic rock (12-0327) are characterized by quartz,  
355 chlorite, sericite and rutile with additionally epidote and calcite present in sample 12-0327. No  
356 ore minerals were recorded in this material.

357 Core from drillhole 2137-16 forms part of the lowermost Carracastle Formation (**Fig.**  
358 **3b**) and is dominated by a chloritized and epidote-altered thick mafic intrusion occurring  
359 structurally below an overlying chloritized crystal tuff. Bleaching and carbonate alteration is  
360 present throughout the hole, but no sulfides were observed.

361 Rocks close to the contact between the Carracastle and Tawnyinagh formations were  
362 tested by drillhole 2137-17 (**Fig. 3a**), and largely comprise an assemblage of altered clastic  
363 rocks and tuffs cut by minor intrusions carrying disseminated pyrite mineralization. Two  
364 samples taken from the core that contained significant base-metal mineralization (12-0336 and

365 12-0341) were examined in thin section. Sample 12-0336 was shown to contain abundant vugs  
366 infilled by quartz and barite. Disseminations of pyrite-sphalerite-galena are seen at the margins  
367 of the vugs with overgrowths of anglesite within in the vug (associated with barite and quartz).  
368 Farther down the hole, sample 12-0341 was taken from a thin quartz veinlet (5mm) containing  
369 intergrown pyrite, chalcopyrite, sphalerite and minor galena. In reflected light, the sphalerite is  
370 characterized by chalcopyrite disease.

371

## 372 4.2 Biostratigraphy

373 The Cummins collection was originally taken from a roadside quarry in the Horan Formation,  
374 ~1 mile SSW of Lurga crossroads (locality A, **Fig. 3a**). This quarry was not located and is  
375 believed to have been destroyed by road development in the area. Cummins (1954) reported  
376 the species in **Table 2**, with the names of the graptolites as revised by Bulman. Dewey et al.  
377 (1970) updated the identifications (**Table 2**). In addition, the brachiopods *Lingulella* and  
378 *Acrotreta* cf. *sagittalis* (Salter) were identified by Cummins (1954), who gave the age as  
379 Arenig. Dewey et al. (1970, p. 30) refined this by restricting age to the Yapeenian Stage of the  
380 Australasian succession, and to the British *Didymograptus hirundo* Zone and the North  
381 American *Isograptus caduceus* Zone.

382

383 The Knock Airport collection obtained here is similar to, but not identical to that of Cummins  
384 (1954). All the taxa listed below were described by Rushton (2014), who reported that although  
385 the graptolites show no observable tectonic deformation, they are mostly fragmentary and  
386 strongly flattened by compaction, and accordingly presented difficulties for identification and  
387 interpretation.

388 *Pseudisograptus* sp. of the *manubriatus* (T.S. Hall) species group (**Fig. 7a**)

389 *Yutagraptus?* *v-deflexus* (Harris) (**Fig. 7b**)

390 *Arienigraptus?* sp. (**Fig. 7e**)

391 *Isograptus caduceus?* cf. *nanus* Ruedemann. (**Fig. 7d**)

392 *Clonograptus* aff. *timidus* Harris & Thomas?

393 Dichograptid and dendroid? fragments

394 *Didymograptus (Expansograptus)* spp. (fragments), including *D. (E.)* aff. *nitidus*  
395 (Hall)

396 *Exigraptus uniformis* Mu (**Fig. 7g-i**)

397 *Pseudophyllograptus* sp.

398 *Skiagraptus gnomicus* (Harris & Keble) (**Fig. 7j-k**)

399 *Tetragraptus* spp.

400 Brachiopods: two species of lingulellids

401

402 According to Rushton (2014), the presence of *Pseudisograptus* of the *manubriatus* group, with  
403 *Exigraptus uniformis* and *Skiagraptus gnomonicus*, support Dewey et al.'s interpretation of a  
404 Yapeenian age (= latest Dapingian of the international scale and late Arenig in the British  
405 regional standard; Cocks et al. 2010). Some of the graptolites identified in the fauna from  
406 Knock Airport, e.g. *Y.?* *v-deflexus* and *Skiagraptus*, resemble species that extend up from the  
407 Yapeenian into the lowest part of the overlying Darriwilian Stage (= latest Arenig), but key  
408 indicators of the Darriwilian, such as *Paraglossograptus tentaculatus* and species of  
409 *Undulograptus*, are not present. The Knock Airport fauna is therefore considered to be referable  
410 to the upper Yapeenian (Ya2) substage of the Australasian succession (Rushton, 2014).

411

#### 412 **4.3 U-Pb Geochronology**

413 Four samples (KGC1-3,5) were chosen for age determination from the fossiliferous section of  
414 the Horan Formation, NW of the airport runway (Locality C in **Fig. 3**). Three samples were  
415 collected from the host stratigraphy (KGC2: banded olive to dark green tuff with mudstone rip  
416 up clasts; KGC3: chloritized quartz feldspar porphyry; KGC5: very coarse volcanic breccia)  
417 while one sample was taken from the pyroxene diorite intrusive body exposed at the base of  
418 the section (KGC1; **Fig. 5**). Samples KGC3 and KGC5 were not collected from the section  
419 illustrated in **Figure 5**, but were collected from higher in the stratigraphy (Irish Grid 47467-  
420 96761 & 47524-96748).

421

#### 422 **LA-ICPMS results**

423 Initial LA-ICPMS U-Pb analysis yielded Concordia ages ranging from  $466 \pm 5$  Ma to  $460 \pm 12$   
424 Ma (**Supplementary Figure 1**), yet with high MSWDs and ages significantly younger than the  
425 biostratigraphic age according to Sadler & Cooper (2009; see discussion) that are likely to be  
426 induced by a component of Pb loss within the zircon populations. However, analysis using laser-  
427 ablation did allow the cores of a number of the zircons to be analysed. Only two inherited  
428 grains were identified - both from sample KGC1 (coarse grained epidote-altered diorite). These  
429 yielded  $^{206}\text{Pb}/^{238}\text{U}$  ages of c. 2765 and 2620 Ma. Given the broad spread of errors in the derived  
430 dates, and the potential to solve discussion concerning the fossil-derived biostratigraphic age,  
431 it was decided to analyse the same zircons using CA-ID-TIMS methods.

432

### 433 **CA-ID-TIMS results**

434 Weighted mean dates inclusive of all single analyses for each sample, demonstrate MSWDs in  
435 excess of that statistically acceptable at the 95% CI (confidence interval) for the given number  
436 of analyses. This indicates scatter within dates in excess of analytical precision that is likely to  
437 be derived from xenocrystic- antecrystic zircon and residual open system behavior (as  
438 identified within the LA-ICPMS data) following the chemical abrasion procedure despite all  
439 data points overlapping with Concordia within their given uncertainty. These factors yield dates  
440 older and younger than the emplacement age of interest respectively. Our preferred age  
441 interpretations for the specific units are derived from weighted mean dates of the youngest  
442 populations with statistically acceptable MSWDs. These correspond to the following dates -  
443 KGC1 pyroxene diorite:  $469.11 \pm 0.61/0.63/0.80$  (n=4; MSWD=0.12); KGC2 banded tuff:  
444  $471.95 \pm 0.22/0.25/0.56$  (n=4; MSWD=1.27); KGC3 quartz-feldspar porphyry:  $471.26 \pm$   
445  $0.20/0.29/0.58$  (n=5; MSWD=1.13); KGC5 volcanic breccia:  $470.82 \pm 0.18/0.27/0.57$  (n=4;  
446 MSWD=1.35) (**Fig. 8**).

447

### 448 **4.4 Geochemistry of the Charlestown Group**

449 The geochemistry of the Charlestown Group is presented in **Figures 9 and 10**. Due to the  
450 extensive hydrothermal alteration present across the Charlestown Group and subsequent  
451 greenschist facies metamorphism, only elements demonstrated to be immobile under such  
452 conditions should be used to elucidate petrogenesis. It has been recognized for some time that  
453 most of the major elements, such as SiO<sub>2</sub>, K<sub>2</sub>O, Na<sub>2</sub>O, CaO, MgO, Fe<sub>2</sub>O<sub>3</sub>, and a number of  
454 trace elements (e.g. Sr, Rb, Ba, Cu, Pb, Zn) are easily mobilized by hydrothermal activity  
455 (MacLean, 1990). Only Al<sub>2</sub>O<sub>3</sub>, TiO<sub>2</sub>, Th, Cr, Co, V, Sc, Ga, the high field strength elements  
456 (HFSE: Zr, Nb, Y, Hf, Ta), and the rare earth elements ( $\pm$  Eu) will remain immobile under such  
457 conditions (Pearce and Cann, 1973; Wood, 1980; MacLean, 1990). Mobile elements are used  
458 here to determine the intensity and style of hydrothermal alteration (see O'Connor, 1987 for a  
459 more detailed account), whereas immobile elements were used to determine tectonic setting  
460 and the magmatic evolution of the Charlestown Group.

461

462 **Immobile element geochemistry:** Samples analyzed from the Horan Formation and lower part  
463 of the Carracastle Formation include basalts which range from tholeiitic (CT114, 12-0327) to  
464 calc-alkaline in affinity (CT112) according to the classification scheme of Barrett and MacLean  
465 (1999; also Ross and Bédard, 2009; **Fig. 9a**). Chondrite normalized rare earth element (REE)  
466 profiles are variable for mafic volcanic rocks (La/Yb 1.05 to 10.0), but steep for all samples of

467 crystal tuff regardless of composition (La/Yb 10.8-14.7; **Fig. 10a-b**). Samples are typically  
468 light rare earth element (LREE)-enriched and have flattish heavy rare earth element (HREE)  
469 profiles. A tholeiitic Zr/Y ratio of 3:1 is exhibited by the basaltic intrusion in drillhole 2137-16  
470 (Sample 12-0339), similar to the extrusive basalts (2.7 to 5.6; CT112 and CT114). These three  
471 samples also have similar chondrite-normalized extended REE-profiles (**Fig. 10b**). A mafic  
472 volcanic breccia from drillhole 2137-14 (sample 12-0326) is the only rock which shows LREE-  
473 depletion relative to the HREE (**Fig. 9d**). Although all mafic rocks analyzed from the  
474 Charlestown Group plot within the calc-alkaline basalt field of Wood (1980; **Fig. 9g**), this  
475 reflects the high Th/HFSE ratios present in the samples analyzed (**Fig. 9e**) – possibly a  
476 consequence of crustal contamination (see discussion). Mafic rocks from Charlestown straddle  
477 the backarc, transitional arc and calc-alkaline arc fields of Cabanis and Lecolle (1989; **Fig. 9f**).

478 The mafic lava and felsic tuffs from drillhole 21-3717 (Carracastle/Tawnyinagh  
479 Formation) are characterized by similar extended-REE profiles to crystal tuffs of the Horan  
480 Formation (**Fig. 10c**). All rocks analyzed from the Charlestown Group display pronounced  
481 negative Nb anomalies and weak negative Y anomalies consistent with their formation above  
482 a subduction zone (**Fig. 10**). One of the samples in drillhole 21-3717 (sample 12-0337) shows  
483 very high Nb/Y (0.9), Zr/Y (24.2; **Fig. 9c**), Th/Yb (6.5) ratios, a moderate La/Yb (8.6) ratio  
484 and displays a broadly U-shaped REE profile (**Fig. 10c**). This U-shaped REE profile together  
485 with high Nb/Y and Zr/Y may indicate mobility of REE and/or Y during alteration.

486 Quartz-feldspar porphyritic rocks consistently plot within the volcanic arc granite field  
487 of Pearce et al. (1984) according to Nb-Y (**Fig. 9b**), Ta-Yb, Rb-Y+Nb and Rb-Ta+Yb  
488 discrimination diagrams, and are of FII to FIIIa affinity (i.e. high field strength element  
489 enriched) according to the VMS fertility plot of Lesher et al. (1986; **Fig. 9c**). All samples of  
490 quartz-feldspar porphyry, and the single sample of pyroxene diorite analyzed, show similar,  
491 strongly fractionated (La/Yb 9.6-14.0), calc-alkaline extended REE profiles with prominent  
492 negative Nb and Ti anomalies, positive Zr anomalies and weakly negative Y anomalies (**Fig.**  
493 **10e-f**).

494

#### 495 **Hydrothermal alteration:**

496 As evident from the petrographic work discussed above, most samples examined from the  
497 Charlestown Group have been hydrothermally altered to some degree. Extrusive rocks have  
498 variable SiO<sub>2</sub>, Fe<sub>2</sub>O<sub>3T</sub>, CaO (to 11.08%), K<sub>2</sub>O (to 4.49%), Na<sub>2</sub>O (down to 0.07%), MgO (to  
499 7.52%) and Ba (to 849ppm) concentrations due: to the infilling of voids by silica, carbonate  
500 and barite; epidote veining in mafic volcanic rocks; and varying degrees of silicification,



501 chloritization, sericitization (associated with Na-loss), hematization and carbonate-alteration.  
502 Only three samples, all from drillhole 2137-17, contain significant amounts of sulfides (>0.1%  
503 S). Base metal concentrations are low in all samples analysed (<0.1% Pb, Cu and Zn) except  
504 for a mafic volcanic rock (12-0341) from drillhole 2137-17, which contains high concentrations  
505 of Zn (3.96%), Pb (1.76%), Cu (635ppm), As (371ppm), Cd (100ppm) and Mo (133ppm). Tin  
506 and W concentrations are low in all samples analyzed (to 1.7ppm and 4ppm respectively).

507 To assess the degree of hydrothermal alteration in volcanic rocks associated with VMS  
508 systems, Large et al. (2001) combined two alteration indices - the Alteration Index (AI) and  
509 Carbonate-Chlorite-Pyrite Index (CCPI) and developed the Box Plot as shown in **Figure 9h**.  
510 Together these indices can be used to document the progressive replacement of sodic feldspar  
511 and volcanic glass by sericite, chlorite, carbonate and pyrite. Most samples from the  
512 Charlestown Group plot within the least altered fields (**Fig. 9h**; also the data of O'Connor,  
513 1987), with only two samples falling on common trends associated with VMS proximal  
514 hydrothermal alteration. Sample 12-0341, a sulfide bearing mafic rock from drillhole 2137-17  
515 (described above) plots along a chlorite-pyrite-(sericite) trend typical of relatively proximal  
516 footwall alteration. Sample 12-0337, a bleached felsic volcanic rock of 'trachytic' composition  
517 (also from drillhole 2137-17) plots near the sericite mineral node indicative of slightly more  
518 distal alteration, and is by comparison more intensely silicified (85.83% SiO<sub>2</sub>). The intensity  
519 of alteration in the upper part of this drillhole indicates it is near a hydrothermal up-flow zone  
520 and represents a prime target area for mineral exploration. This is consistent with the presence  
521 of elevated base and trace metal concentrations these samples (described above). Although the  
522 data of O'Connor (1987) is limited, there is a broad correlation between Zn concentration and  
523 Alteration Index values in both quartz-feldspar and feldspar porphyritic rocks.

524

## 525 **5. Discussion**

### 526 **5.1 Evolution of the Charlestown Group and implications for regional correlations**

527 In **Figure 2** our current understanding of the Grampian event as it applies to the northern British  
528 and Irish Caledonides was presented. Early formation of the Deer Park and Highland Border  
529 ophiolites (between the outriding blocks and the Laurentian margin; **Fig. 2a**) was followed by  
530 obduction of these ophiolites (Chew et al., 2010), subduction reversal and the formation of the  
531 Lough Nafoeoy arc system from c. 490 Ma (Draut et al., 2004; **Fig. 2b**). Using the timescale  
532 of Sadler et al. (2009), 'hard' collision of the Lough Nafoeoy arc with the Laurentian margin  
533 in western Ireland (**Fig. 2c**) is constrained to between c. 484 Ma and 476 Ma (based on  
534 graptolite biostratigraphy from the Knock Kilbride and Mt. Partry formations). This occurred

535 around the same time as the exhumation of the Deer Park ophiolitic melange at  $482 \pm 1$  Ma  
536 (Chew et al., 2010), with ophiolitic detritus recorded in the younger Letterbrock Formation  
537 (Wrafter and Graham, 1989, Dewey and Mange, 1999; **Fig. 11**).

538 In Northern Ireland, the obduction of the Tyrone arc (=Tyrone Volcanic Group) and its  
539 associated ophiolite (=Tyrone Plutonic Group) to an outboard microcontinental block (=Tyrone  
540 Central Inlier) occurred prior to c. 470 Ma (Hutton et al., 1985; Cooper et al., 2011; Hollis et  
541 al., 2013b, **Fig. 2d**), though most likely not before c. 473 Ma (due to the absence of xenocrystic  
542 zircons in the Formil rhyolite: Cooper et al., 2008). In western Scotland, a Ca4 to Ya1  
543 (Ca=Castlemanian, Ya=Yapeenian) age was obtained for a graptolite fauna from the North  
544 Ballaird borehole (references in Stone, 2014). This clastic sequence contains granules of  
545 altered serpentine with algal rims in one of these late Arenig beds, implying ophiolitic material  
546 at Ballantrae was available for erosion and incorporation by c. 472 Ma (**Fig. 11**). This is in  
547 agreement with K-Ar dating of the metamorphic sole of the Ballantrae ophiolite ( $478 \pm 8$  Ma:  
548 Bluck et al., 1980). The Charlestown Group (ca. 470 Ma, *this study*) clearly fits within the later  
549 stages of the Grampian event (**Fig. 11**), and developed after the first two stages of arc-ophiolite  
550 accretion (i.e. Deer Park/Highland Border, and Lough Nafooe). Its relationship to the  
551 Tyrone/Ballantrae arc system, and syn-collisional stage of the Lough Nafooe arc (i.e.  
552 Tourmakeady Group) will be discussed below.

553 Whole rock geochemical data from the c. 472-469 Ma Charlestown Group are  
554 consistent with its formation as part of a peri-Laurentian affinity volcanic arc, in a similar  
555 tectonic setting to the Tyrone and Ballantrae arcs (**Fig. 2d**). Early magmatism generated the  
556 tholeiitic and calc-alkaline mafic rocks of the Horan Formation and lower part of the  
557 Carracastle Formation (e.g. drillhole 2737-14). These are interbedded with mafic volcanic  
558 breccias, crystal tuff and sedimentary rocks (chert, siltstone and mudstone). Overlying deposits  
559 of the upper Carracastle and Tawnyinah formations are dominated by LILE- and LREE-  
560 enriched, calc-alkaline andesitic and felsic volcanoclastic rocks respectively. Together these  
561 three formations record the evolution of the Charlestown Group, from a relatively juvenile arc  
562 system in a deep marine setting to a progressively more mature, fractionated, volcanoclastic  
563 dominated successions. High Th/Yb ratios for calc-alkaline volcanic/volcanoclastic rocks  
564 suggest the Charlestown arc was founded upon continental crust (either composite Laurentian  
565 margin or microcontinental block), supported by the presence of inherited zircons ( $>2$  Ga) in  
566 sample KGC1 (intrusive pyroxene diorite). The Horan Formation yields U-Pb zircon dates of  
567 between 472 and 469 Ma (Fig. 7). The Carracastle and Tawnyinah formations remain undated,  
568 but are stratigraphically younger than the volcanoclastic rocks of the Horan Formation (470.82

569  $\pm 0.57$  Ma). A geochemical comparison of extended REE profiles from the Charlestown Group  
570 to the arc sequences of western Ireland (i.e. Lough Nafooy, Tourmakeady and Murrisk  
571 groups) and Northern Ireland (the Tyrone Igneous Complex) is presented in **Figure 10**. Rare  
572 LREE-depleted volcanic breccias at Charlestown (sample 12-0326) are similar to those of the  
573 Beaghmore Formation of the lower Tyrone Volcanic Group and less so to the  $>490$  Ma  
574 Bencorragh Formation of the lower Lough Nafooy Group (**Fig. 10d**). A correlation can be  
575 ruled out with both formations on the basis of age constraints presented here (**Fig. 11**). Similar  
576 rocks (island arc, LREE-depleted tholeiitic basalts) also occur in the juvenile Ballantrae arc  
577 sequences, which are poorly constrained by Sm-Nd ages with large errors (Thirlwall and Bluck,  
578 1984; **Fig. 11**). Large ion lithophile element (LILE) enriched volcanic/volcaniclastic rocks  
579 which comprise most the Charlestown Group stratigraphy are geochemically similar to those  
580 of the Tourmakeady, Murrisk and Tyrone Volcanic groups (**Fig. 10a-c**). No Fe-Ti enriched  
581 mafic rocks of eMORB affinity have been recognized in the Charlestown Group or other  
582 western Ireland sequences. These lavas are common in the c.475-474 Ma lower Tyrone  
583 Volcanic Group, less so in the c. 469 Ma uppermost Tyrone Volcanic Group (Hollis et al.,  
584 2012), and abundant at Ballantrae (the 'within plate' lavas of Stone, 2014 and earlier workers).  
585 Data for the Tourmakeady Group is shown on Fig. 10b where it is comparable to Charlestown.  
586 The Delaney Dome Formation (not shown in **Fig. 11**) represents a tectonic window through  
587 the continental arc intrusive rocks of Connemara, western Ireland. A U-Pb zircon age of  $474.6$   
588  $\pm 5.5$  Ma presented by Draut and Clift (2002) is within error of the Charlestown Group. Its  
589 LREE-enrichment and trace element characteristics are most similar to the c 475 Ma  
590 Tourmakeady Group (see Draut and Clift, 2002) and these authors consider the Delaney Dome  
591 Formation and Tourmakeady Group to be along-strike equivalents.

592         Syn- to post-continental arc intrusive rocks which are of similar age to the Charlestown  
593 Group (c. 470 Ma) occur in Co. Tyrone (the late arc intrusive suite of the Tyrone Igneous  
594 Complex: Cooper et al., 2011), Co. Sligo (Sliswood Division: Flowerdew et al., 2005) and  
595 Connemara (Friedrich et al., 1999a,b; Draut et al., 2002) (**Figs. 1,11**). Chondrite normalized  
596 REE profiles for QFP intrusive rocks from the Charlestown Group are geochemically similar  
597 to samples of c. 465 Ma quartz-feldspar porphyritic dacite and c. 467-464 Ma granite which  
598 intrudes the upper levels of the Tyrone Igneous Complex (Draut et al. 2009; Cooper et al. 2011;  
599 **Fig. 10e**). The single sample of pyroxene diorite analyzed from Charlestown (CT105) also  
600 displays a similar chondrite normalized extended REE-profile, falling within the range of  
601 compositions present for c. 470-465 Ma diorites which intrude the Tyrone Igneous Complex  
602 (**Fig. 10f**). The slightly younger age of the pyroxene diorite (KGC1: c. 469 Ma) than all other

603 dated rocks of the Charlestown Group (**Fig. 8**) is consistent with its intrusive nature. Zircon  
604 inheritance is also a common feature in late (post 470 Ma) intrusive rocks of the Tyrone Igneous  
605 Complex (Hutton et al., 1985; Cooper et al., 2011; Hollis et al., 2012, 2013a), with zircons  
606 most likely inherited from the underlying Tyrone Central Inlier - a possible outboard  
607 Laurentian-affinity microcontinental block (Chew et al., 2008). The geochemistry of the syn-  
608 to post-collisional continental arc intrusives of Connemara has been presented by Draut et al.  
609 (2002). All samples show LREE enrichment, with comparable La/Sm ratios to the  
610 Tourmakeady Group. No geochemical data is available for the Sliswood intrusive rocks  
611 (Flowerdew et al., 2005). The presence of syn- post- collisional intrusive rocks in Dalradian  
612 sequences of Laurentian margin confirms the sequence of arc-continent collision and continued  
613 northward dipping subduction post 470 Ma.

614         Based on the above, we favour a correlation between the Charlestown Group and the  
615 late (i.e. post-subduction flip) arc sequences of the Irish Caledonides – particularly the late  
616 development of the upper Tyrone Volcanic Group (i.e. post accretion Broughderg Formation),  
617 and the late c. 470-457 Ma continental arc intrusive rocks of these accreted terranes: Co. Tyrone  
618 ( $470.3 \pm 1.9$  to  $464.9 \pm 1.5$  Ma: Draut et al., 2009; Cooper et al., 2011), Connemara ( $474.5 \pm$   
619  $1.0$  Ma to  $462.5 \pm 1.2$  Ma: Friedrich et al., 1999a,b), Co. Sligo ( $474 \pm 5$  Ma to  $467 \pm 6$  Ma:  
620 Flowerdew et al., 2005). Continental arc intrusive rocks also intruded the Dalradian sequences  
621 of eastern Scotland until to  $457 \pm 1$  Ma (Oliver et al., 2000, 2008; Carty et al., 2013). Although  
622 a correlation to the youngest stage of the Tourmakeady Group (i.e. uppermost Tourmakeady  
623 and Srah formations) cannot be ruled out based on our geochronology and the geochemistry of  
624 tuffs and felsic volcanic rocks, the presence of abundant subaqueous and geochemically  
625 juvenile mafic rocks at Charlestown is difficult to reconcile a syncollisional tectonic setting (as  
626 is the presence of VMS mineralization, typically associated with rifted arc or backarc settings  
627 – see section 5.3.).

628

## 629 **5.2 Implications for the Middle Ordovician timescale**

630 Despite its importance, there are relatively few U-Pb constraints for the Early to Middle  
631 Ordovician timescale (Cooper and Sadler, 2012; Lindskog et al. 2016). Based on the fauna  
632 recovered from the Knock Airport sequence, the upper part of the Horan Formation is  
633 correlated with the Upper Yapeenian or Ya2 stage of the Australian succession (i.e. late  
634 Dapingian global stage / Late Arenig) (Ruston, 2014; **Fig. 12**). Together with the new CA-ID-  
635 TIMS ages presented here, this site represents an important new constraint for calibrating the  
636 Middle Ordovician timescale.

637 Sadler et al. (2009) assessed the duration of the Yapeenian Stage as less than 2 Ma,  
638 with Ya2 lasting from 471.21 to 470.54 Ma (**Fig. 12**). This was based on calibration points  
639 bracketing the interval at  $486.78 \pm 2.57$  Ma,  $481.13 \pm 2.76$  Ma,  $469 \pm 6.00$  Ma and  $465.46 \pm$   
640  $3.53$  Ma (total  $2\sigma$  uncertainty; Schmitz, 2012). The Ordovician timescale was later revised by  
641 Cooper and Sadler (2012) who modified the duration of Ya2 to a period from 467.7 to 467.3  
642 Ma, significantly younger than that of Sadler et al. (2009) and inconsistent with the combined  
643 graptolite and U-Pb constraints presented here. It is important to note that this revised  
644 Ordovician timescale included a calibration point based on the correlation of a U-Pb zircon age  
645 of  $473 \pm 1$  Ma from the Formil rhyolite (Tyrone Igneous Complex) with a Cal graptolite fauna  
646 from Slieve Gallion (as described in Cooper et al., 2008). This proposed correlation between  
647 the Formil rhyolite and volcanic succession on Slieve Gallion (Cooper et al. 2008) has now  
648 been shown to be incorrect based on recent mapping and geochemistry (Hollis et al., 2013a).  
649 The erroneously correlated c. 473 Ma age clearly pushes the Floian part of the Cooper and  
650 Sadler (2012) chart to younger ages with the point lying above their calibration line (point O3  
651 on their Fig. 20.11). This is confirmed by the recent study of Lindskog et al. (2016) who report  
652 a U-Pb zircon date of  $467.50 \pm 0.28$  Ma from the distinct 'Likhall' meteorite bed of Sweden.  
653 Lindskog et al. (2016) provide a revised Middle Ordovician timescale for the Darriwilian  
654 global stage and suggest that the base of the Darriwilian, presently cited as  $467.3 \pm 1.1$  Ma  
655 must be moved back in time. However, this refined timescale of Lindskog et al. (2016; **Fig. 12**)  
656 still includes the erroneous correlation of the Formil age to the graptolite bearing sequence at  
657 Slieve Gallion (Cooper et al., 2008). Limitations with the late Cambrian to Early Ordovician  
658 section of the International Chronostratigraphic Charts have been discussed by Landing et al.  
659 (2015).

660 Our four U-Pb ages of  $471.95 \pm 0.56$  Ma,  $471.26 \pm 0.58$  Ma,  $470.82 \pm 0.57$  and  $469.11$   
661  $\pm 0.80$  Ma ( $2\sigma$  total uncertainty) for the Knock Airport sequence of the Horan Formation are  
662 in agreement with the original Sadler et al. (2009) duration of the Ya2 stage of the earlier  
663 Dapingian (471.21 to 470.54 Ma). The Knock Airport sequence of latest Dapingian (Ya2) age  
664 is well constrained by sample KGC2 (banded tuff;  $471.95 \pm 0.56$  Ma; **Fig. 5**) which underlies  
665 the graptolite bearing horizon and samples KGC3 and KGC5 (**Fig. 5, 7**) which overlie it. The  
666 younger age of  $469.11 \pm 0.80$  Ma is from a pyroxene diorite that intrudes the sequence. We  
667 suggest that the Formil rhyolite age be removed from all future Ordovician calibrations, with  
668 the Lindskog et al. (2016) age providing an important constraint for the lower Darriwilian, and  
669 the Knock Airport fauna for the latest Dapingian (**Fig. 12**). The newly presented geochronology  
670 for the Knock Airport sequence, provides a significant refinement of the existing  $469 \pm 6.00$

671 Ma Dapingian constraint, determined from a rhyolite of the Cutwell Group, central  
672 Newfoundland (Dunning and Krogh, 1991).

673

### 674 **5.3 Regional mineral potential**

675 From the work presented here it is evident that the Charlestown Cu deposit is not consistent  
676 with ‘porphyry copper’ style mineralization (e.g. Berger et al., 2008), as stated by O’Connor  
677 and Poustie (1986). Breccia textures, the nature of hydrothermal alteration and the style of  
678 mineralization (**Fig. 4**) are more consistent with a VMS system. Volcanogenic massive sulfide  
679 deposits develop in volcanic sequences undergoing extension, as metal bearing hydrothermal  
680 fluids are focused from depth and mix with ambient seawater to precipitate sulfides at or below  
681 the seafloor (Franklin et al., 2005). In Phanerozoic rocks, VMS deposits are typically restricted  
682 to arc, ophiolite and backarc sequences (reviewed in Piercey, 2011). Despite their abundance  
683 in accreted arc and ophiolite terranes of the Newfoundland Appalachians (van Staal, 2007;  
684 Piercey, 2007), few VMS deposits have been recognized in the British and Irish Caledonides  
685 (Hollis et al., 2014). Economic deposits identified to date are restricted to peri-Gondwanan  
686 affinity arc and backarc terranes south of the Iapetus Suture, such as at Avoca and Parys  
687 Mountain (Hollis et al., 2014).

688 Evidence presented here and in O’Connor (1987) suggests that the entire volcanic  
689 stratigraphy of the Charlestown Group was deposited in a submarine arc environment. This  
690 includes the repeated occurrence of deep sea sedimentary rocks (i.e. mudstone, jasper, chert)  
691 throughout all three formations, and the presence of interbedded, well stratified tuffs with arc  
692 like geochemical characteristics (**Figs. 9,10**). Furthermore, where the quartz-feldspar  
693 porphyritic rocks are observed in outcrop, breccia textures are consistent with peperite,  
694 autobrecciation and hydraulic fracturing (section 4.4.2). This suggests these thin units were  
695 emplaced as high-level synvolcanic sills into unconsolidated wet sediments and tuffs just below  
696 the seafloor. Localized occurrences of crystal tuff occur where these magmas were erupted.

697 Hydrothermal activity is well developed throughout the Charlestown Cu deposit (**Fig.**  
698 **4**), and also throughout the entire sequence. The concentric zoning of alteration assemblages  
699 associated with the Charlestown mineralization only superficially resembles that of porphyry  
700 Cu deposits worldwide; which typically encompass a potassic core surrounded by concentric  
701 phyllic and propylitic shells (Lowell and Guilbert, 1970). The characteristic potassic alteration  
702 from porphyry Cu style mineralization is absent at Charlestown, and furthermore the patchy  
703 hematitic alteration is not usually recorded in porphyry copper systems (O’Connor and Poustie  
704 1986). O’Connor and Poustie (op. cit.) unconvincingly suggest the silicic and sericitic

705 alteration seen at Charlestown represents the phyllic core associated with porphyry systems,  
706 whilst localized clay rich alteration to argillic zones, and chloritic alteration to propylitic zones.  
707 This type of alteration is much more typical for VMS systems (Franklin et al. 2005)

708         Within the Charlestown Cu deposit, the intense zone of chloritic alteration appears to  
709 be restricted underneath the deposit, and increases in thickness below the zone of pyrite-  
710 chalcopyrite mineralization (**Fig. 4**). This, together with the presence of a central core of  
711 silicification already discussed, is consistent with VMS systems, particularly feeder zones (e.g.  
712 Franklin et al., 2005) which will be characterized by stockwork like ‘type 4’ brecciation and  
713 base metal mineralization caused by hydraulic fracturing. A broader halo of sericitic-chloritic  
714 alteration is consistent with the more distal portions of felsic-hosted VMS systems (Yeats et  
715 al., 2017). The development of similar alteration assemblages in the hanging-wall of the deposit  
716 (**Fig. 4**), together with localized ‘type 1’ peperite development with ash tuffs, suggests that  
717 mineralization occurred sub-seafloor and was predominantly replacive. Minor exhalation is  
718 indicated by the presence of unmineralized jaspers (see following). The concentration of  
719 sphalerite-barite and sphalerite-galena-barite mineralization towards the periphery of the  
720 deposit (**Fig. 4**) is also consistent with VMS systems (Franklin et al., 2005). Further evidence  
721 for VMS activity includes the observation of ‘chalcopyrite disease’ (Barton and Bethke, 1987)  
722 in many samples from across the volcanic inlier, and the presence of significant sphalerite  
723 mineralization in drillhole 2137-17 (3.96 wt% Zn, 635 ppm Cu) in the upper Carracastle  
724 Formation (sample 12-0341; **Fig. 3b**).

725         Cathelineau (1988) proposed an empirical chlorite mineral geothermometer where  
726 formation temperature  $T(^{\circ}\text{C}) = -61.92 + 321.98(\text{Al}_{\text{(IV)}})$ .  $\text{Al}_{\text{(IV)}}$  can be calculated from SEM  
727 analysis and substituted to derive formation temperature (Stobbs 2013). Results from sample  
728 CT206, a felsic breccia from the Carracastle Formation, indicates temperatures ranging  
729 between 340°C - 395°C, within the range for formation conditions for a VMS deposit,  
730 equivalent to higher greenschist metasomatic conditions, and importantly well below  
731 temperatures associated with porphyry copper deposits (reviewed in Berger et al., 2008). Most  
732 rocks from the Charlestown Group display at least some evidence for seawater interaction, such  
733 as calcite amygdales in mafic lavas (e.g. 12-0327) or voids associated with autobrecciation  
734 infilled with barite, calcite and quartz (CT206; **Fig. 6b**). In sample CT113, a crystal tuff from  
735 the Horan Formation, SEM results show some form of iron oxide with 200 ppm copper  
736 associated with chlorite (**Fig. 6a**). The texture of the chlorite is most likely explained by the  
737 precipitation in voids from a silica-rich hydrothermal fluid.

738 Sample 12-0336 from drillhole 2137-17 (upper Carracastle Formation), contains vuggy  
739 quartz in association with barite implying hydrothermal activity similar in nature to the above  
740 samples. Anglesite [PbSO<sub>4</sub>], an oxidation product of galena, was also observed. The oxidation  
741 of this phase could be associated with the apron zone of a VMS deposit, which is normally  
742 characterized by oxidized ore minerals along with barite and hematite and iron-rich cherts and  
743 jaspers (Herrington et al., 2005; Hollis et al., 2015; Ayupova et al. 2016), similar to the  
744 successions found at the top hole 2137-14 but also comparable to sample CT113, with copper  
745 rich hematite and barite. Large blocks of jasper float were noted by the authors north of Knock  
746 Airport, similar in appearance to that associated with hydrothermal alteration and base metal  
747 occurrences in the Tyrone Igneous Complex (Hollis et al., 2015, 2016). Such jaspers may form  
748 as silica-iron gels, precipitated from the non-buoyant parts of hydrothermal plumes or through  
749 the replacement of the volcanic stratigraphy (Hollis et al., 2015).

750 Together these results indicate that the mineralization at Charlestown is more consistent  
751 with a VMS system than a porphyry copper deposit (**Fig. 13**). The link established herein to  
752 the Tyrone Igneous Complex further highlights the VMS prospectivity of the Charlestown area.  
753 In the Tyrone Igneous Complex numerous sub-economic Cu-Pb-Zn-Ag-Au occurrences have  
754 been identified, associated with locally intense hydrothermal activity (Hollis et al., 2014). Most  
755 base metal mineralization is restricted to the uppermost Tyrone Volcanic Group of similar age  
756 (c. 473-469 Ma; Hollis et al., 2012) to the Charlestown Group. Sub-economic VMS-style  
757 mineralization in Co. Tyrone is predominantly associated with silicified and variably  
758 sericitized and chloritized felsic tuffs, flows and rhyolite domes (Hollis et al., 2016).

759

## 760 CONCLUSIONS

761 We have reassessed the role of the Charlestown Group in the context of the c. 474-465 Ma  
762 Grampian orogeny, based on new fieldwork, high-resolution airborne geophysics, graptolite  
763 biostratigraphy, U-Pb zircon dating, whole rock geochemistry, and an examination of historic  
764 drillcore from across the volcanic inlier. The Charlestown Group has been divided into three  
765 formations: Horan, Carracastle, Tawnyinah. The Horan Formation comprises a mixed  
766 sequence of tholeiitic to calc-alkaline basalt, crystal tuff and sedimentary rocks (e.g. black  
767 shale, chert), forming within an evolving peri-Laurentian affinity island arc. The presence of  
768 graptolites *Pseudisograptus* of the *manubriatus* group and the discovery of *Exigraptus*  
769 *uniformis* and *Skiagraptus gnomonicus* favour a Yapeenian (= late Arenig; Ya2 stage) age for  
770 the Horan Formation (equivalent to c. 471.2-470.5 Ma according to the timescale of Sadler et  
771 al., 2009). Together with three new U-Pb zircon ages of ca. 471.95-470.82 Ma from enclosing



772 felsic tuffs and volcanic breccias, this fauna provides an important new constraint for  
773 calibrating the Middle Ordovician timescale. Overlying deposits of the Carracastle and  
774 Tawnyinah formations are dominated by LILE- and LREE-enriched calc-alkaline andesitic  
775 tuffs and flows, coarse volcanic breccias and quartz-feldspar porphyritic intrusive rocks,  
776 overlain by more silicic tuffs and volcanic breccias with rare occurrences of sedimentary rocks.  
777 The relatively young age for the Charlestown Group in the Grampian orogeny, coupled with  
778 high Th/Yb and zircon inheritance (c. 2.7 Ga) in intrusive rocks indicate the arc was founded  
779 upon continental crust (either composite Laurentian margin or microcontinental block).  
780 Regionally, this best correlates with the post-subduction flip volcanic/intrusive rocks of the  
781 Irish Caledonides, specifically the late-stage development of the Tyrone Igneous Complex,  
782 Murrisk Group ignimbrites, the late intrusive rocks of Connemara (western Ireland) and the  
783 Slishwood Division in Co. Sligo. Breccia textures and mineralization is incompatible with the  
784 porphyry hypothesis for the genesis of the Charlestown copper deposit and this study suggests  
785 that features are more consistent with a volcanogenic massive sulfide (VMS) deposit.

786

## 787 **ACKNOWLEDGEMENTS**

788 The authors would like thank Quentin Crowley (Trinity College Dublin) for zircon separation,  
789 Emma Williams and Stanislav Strekopytov (NHM) for helping with whole rock geochemistry,  
790 and Anton Kearsley and Will Brownscombe (NHM) for SEM assistance. Tom McIntyre is also  
791 thanked for access to drillcore at the GSI. Part of this work formed Iain Stobbs' MSci thesis at  
792 Imperial College London. Stephen Daly and John Dewey are thanked for many thoughtful  
793 discussions on the geology of the Charlestown Group. RJH publishes with the permission of  
794 the NHM. MRC and ST publish with permission of the Executive Director of the BGS (NERC).  
795 SPH and BMcC publish with permission of the Director of the GSI. SPH is currently supported  
796 by the Geological Survey Ireland/DCCAIE Postdoctoral Fellowship Programme (No. 2016-PD-  
797 003), hosted at the Irish Centre for Research in Applied Geosciences (iCRAG). iCRAG is  
798 funded under the Science Foundation Ireland Research Centres Programme and is co-funded  
799 under the European Regional Development Fund. The Tellus Border project was funded by the  
800 INTERREG IVA program of the European Regional Development Fund, which is managed by  
801 the Special EU Programs Body. The project was additionally part-funded by Oriel Selection  
802 Trust Ltd, the Department of Environment, Community and Local Government  
803 (Ireland) and Department of the Environment (Northern Ireland). The authors thank the  
804 reviewers for their constructive comments and greatly improving the manuscript.

805

806

807 **References**

- 808 Ayupova, N.R., Maslennikov, V.V., Tessalina, S.G., Shilovsky, O.P., Sadykov, S.A., Hollis,  
809 S.P., Danyushevsky, L.V., Safina, N.P. & Statsenko, E.O., 2016, Tube fossils from  
810 gossanites of the Urals VHMS deposits, Russia: authigenic mineral assemblages and trace  
811 element distributions. *Ore Geology Reviews*. DOI: 10.1016/j.oregeorev.2016.08.003
- 812 Barton, P.B. Jr & Bethke, P.M, 1987, Chalcopyrite disease in sphalerite: pathology and  
813 epidemiology. *American Mineralogist*, **72**, 451-467.
- 814 Berger, B.R., Ayuso, R.A., Wynn, J.C. & Seal, R.R., 2008, Preliminary model of porphyry  
815 copper deposits. U.S. Geological Survey Open-File Report 2008-1321, 55p.
- 816 Bluck, B.J., Halliday, A.N., Aftalion, M. & Macintyre, R.M., 1980, Age and origin of  
817 Ballantrae ophiolite and its significance to the Caledonian orogeny and Ordovician time  
818 scale. *Geology*, **8**, 492-495.
- 819 Cabanis, B. & Lecolle, M., 1989, Le diagramme La/10-Y/15-Nb/8; un outil pour la  
820 discrimination des series volcaniques et al mise en evidence des processus de mélange et/ou  
821 de contamination crustale. The La/10-Y/15-Nb/8 diagram; a tool for distinguishing volcanic  
822 series and discovering crustal mixing and/or contamination. *Comptes Rendus de l'Academie  
823 des Sciences, Serie 2, Mecanique, Physique, Chimie, Sciences de l'Univers, Sciences, de la  
824 Terre*, **309**, 2023-2029.
- 825 Carty, J.P., Connelly, J.N., Hudson, N.F.C. & Gale, J.F.W., 2013, Constraints on the timing of  
826 deformation, magmatism and metamorphism in the Dalradian of NE Scotland. *Scottish  
827 Journal of Geology*, **48**, 103-117.
- 828 Cathelineau, M., 1988, Cation site occupancy in chlorites and illites as a function of  
829 temperature. *Clay Minerals*, **23**, 471-485
- 830 Charlesworth, H.A.K., 1960, The Lower Palaeozoic inlier of the Curlew Mountain anticline.  
831 *Proceedings of the Royal Irish Academy*, **61B**, 37-50.
- 832 Chew, D.M., 2009. Grampian orogeny, in Holland, C.H. & Saunders, A.D. (eds) *The Geology  
833 of Ireland. 2nd edition*, 69-93.
- 834 Chew, D. & Stillman, C.J., 2009, Late Caledonian orogeny and magmatism. *In*: Holland, C. H.  
835 & Saunders, I. S. (eds) *The Geology of Ireland*. Second edition, 143-173.
- 836 Chew, D.M., Graham, J.R. & Whitehouse, M.J., 2007. U-Pb zircon geochronology of  
837 plagiogranites from the Lough Nafoeey (= Midland Valley) arc in western Ireland:  
838 constraints on the onset of the Grampian orogeny. *Journal of the Geological Society,  
839 London*, **164**, 747-750.

- 840 Chew, D.M., Flowerdew, M.J., Page, L.M., Crowley, Q.G., Daly, J.S., Cooper, M. R. &  
841 Whitehouse, M.J., 2008. The tectonothermal evolution and provenance of the Tyrone  
842 Central Inlier, Ireland: Grampian imbrication of an outboard Laurentian microcontinent?  
843 *Journal of the Geological Society, London*, **165**, 675-685.
- 844 Chew, D.M., Daly, J.S., Magna, T., Page, L.M., Kirkland, C.L., Whitehouse, M.J. & Lam, R.,  
845 2010, Timing of ophiolite obduction in the Grampian orogen. *Geological Society of America*  
846 *Bulletin*, **122**, 1787-1799.
- 847 Clift, P.D. & Ryan, P.D., 1994. Geochemical evolution of an Ordovician island arc, South  
848 Mayo, Ireland. *Journal of the Geological Society, London*, **151**, 329-342.
- 849 Clifford, J.A., Earls, G., Meldrum, A.H. & Moore, N., 1992, Gold in the Sperrin Mountains,  
850 Northern Ireland: an exploration case history. In: Bowden, A.A., Earls, G., O'Connor, P.G.  
851 & Pyne, J.F. (eds) *The Irish Minerals Industry 1980-1990*. Irish Association for Economic  
852 Geology, Dublin, pp 77-87
- 853 Cocks, L. R. M., Fortey, R. A. & Rushton, A. W. A. 2010. Correlation for the Lower  
854 Palaeozoic. *Geological Magazine*, **147**, 171-180.
- 855 Condon, D.J., Schoene, B., McLean, N.M., Bowring, S.A., & Parrish, R.R., 2015. Metrology  
856 and traceability of U–Pb isotope dilution geochronology (EARTHTIME Tracer Calibration  
857 Part I). *Geochimica et Cosmochimica Acta* 164, 464–480. doi:10.1016/j.gca.2015.05.026
- 858 Cooper, M.R., Crowley, Q.G. & Rushton, A.W.A., 2008. New age constraints for the  
859 Ordovician Tyrone Volcanic Group, Northern Ireland. *Journal of the Geological Society,*  
860 *London*, **165**, 333-339.
- 861 Cooper, M.R., Crowley, Q.G., Hollis, S.P., Noble, S.R., Roberts, S., Chew, D., Earls, G.,  
862 Herrington, R. & Merriman, R.J., 2011. Age constraints and geochemistry of the Ordovician  
863 Tyrone Igneous Complex, Northern Ireland: implications for the Grampian orogeny.  
864 *Journal of the Geological Society, London*, **168**, 837-850.
- 865 Cooper, M.R., Crowley, Q.G., Hollis, S.P., Noble, S.R. & Henney, P.J., 2013, A U-Pb age for  
866 the Late Caledonian Sperrin Mountains minor intrusions suite in the north of Ireland: timing  
867 of slab break-off in the Grampian terrane and the significance of deep-seated, crustal  
868 lineaments. *Journal of the Geological Society*, **170**, 603-614.
- 869 Cooper, M.R. & Mitchell, W.I., 2004. Midland Valley Terrane, in Mitchell, W.I. (ed)., *The*  
870 *Geology of Northern Ireland. Our Natural Foundation, second edition*. Geological Survey  
871 of Northern Ireland.
- 872 Cooper, R.A. & Sadler, P.M., 2012, The Ordovician Period. In: Gradstein, F.M., Ogg, J.G.,  
873 Schmitz, M. & Ogg, G. (eds.) *The Geologic Time Scale 2012*. Elsevier B.V.

874 Crowley, Q.G. & Strachan, R.A., 2014, U-Pb zircon constraints on obduction initiation of the  
875 Unst Ophiolite: an oceanic core complex in the Scottish Caledonides? *Journal of the*  
876 *Geological Society, London*, **172**, 279-282.

877 Cummins, W. A., 1954. An Arenig volcanic series near Charlestown, Co. Mayo. *Geological*  
878 *Magazine*, 91, 102-104.

879 DePaolo, D.J., 1981, Trace element and isotopic effects of combined wallrock assimilation and  
880 fractional crystallization. *Earth and Planetary Science Letters*, **53**, 189-202.

881 DePaolo, D.J. & Wasserburg, G.J., 1976, Nd isotopic variations and petrogenetic models.  
882 *Geophysical Research Letters*, **3**, 249-252.

883 Dewey, J.F., 2005, Orogeny can be very short. *PNAS*, **102**, 15286-15293.

884 Dewey, J.F. & Mange, M.A., 1999, Petrography of Ordovician and Silurian sediments in the  
885 western Irish Caledonides: tracers of a short-lived Ordovician continent-arc collision  
886 orogeny and the evolution of the Laurentian Appalachian-Caledonian margin. *In:*  
887 MacNiocaill, C. & Ryan, P.D., (eds), *Continental Tectonics*. Geological Society of London,  
888 Special Publication, **164**, 55-107.

889 Dewey, J.F. & Shackleton, R.M., 1984, A model for the evolution of the Grampian tract in the  
890 early Caledonides and Appalachians. *Nature*, **312**, 115-121.

891 Dewey, J. F., Rickards, R. B. & Skevington, D., 1970. New light on the age of Dalradian  
892 deformation and metamorphism in western Ireland. *Norsk geologisk Tidsskrift*, **50**, 19-44.

893 Draut, A.E. & Clift, P.D., 2002, The origin and significance of the Delaney Dome Formation,  
894 Connemara, Ireland. *Journal of the Geological Society, London*, **159**, 95-103.

895 Draut, A.E., Clift, P.D., Hannigan, R.E., Layne, G. & Shimizu, N., 2002, A model for  
896 continental crust genesis by arc accretion: rare earth element evidence from the Irish  
897 Caledonides. *Earth and Planetary Science Letters*, **203**, 861-877.

898 Draut, A.E., Clift, P.D., Chew, D.M., Cooper, M.J., Taylor, R.N. & Hannigan, R.E., 2004,  
899 Laurentian crustal recycling in the Ordovician Grampian Orogeny: Nd isotopic evidence  
900 from western Ireland. *Geological Magazine*, **141**, 195-207.

901 Draut, A.E., Clift, P.D., Amato, J.M., Blusztajn, J. & Schouten, H., 2009, Arc-continent  
902 collision and the formation of continental crust: a new geochemical and isotopic record from  
903 the Ordovician Tyrone Igneous Complex, Ireland. *Journal of the Geological Society,*  
904 *London*, **166**, 485-500.

905 Dunning, G.R. & Krogh, T.E., 1991. Stratigraphic correlation of the Appalachian orogeny using  
906 advances U-Pb zircon geochronology techniques. *In:* Barnes, C.R. & Williams, S.H. (Eds.)

907 Fifth International Symposium on the Ordovician system. Geological Survey of Canada  
908 Paper 90-09, Ottawa, 85-92.

909 Earls, G., Hutton, D.W.H., Wilkinson, J., Mole, N., Parnell, J., Fallick, A. & Boyce, A., 1996,  
910 The gold metallogeny of northwest Northern Ireland. Geological Survey of Northern Ireland  
911 Technical Report 96/6, 107pp.

912 Flowerdew, M.J., Daly, J.S. & Whitehouse, M.J., 2005, 470 Ma granitoid magmatism  
913 associated with the Grampian Orogeny in the Sliswood Division, NW Ireland. *Journal of*  
914 *the Geological Society, London*, **162**, 563-575.

915 Franklin, J.M., Gibson, H.L., Galley, A.G. & Jonasson, I.R., 2005. Volcanogenic massive  
916 sulfide deposits. In: Hedenquist, J.W., Thompson, J.F.H., Goldfarb, R.J. & Richards, J.P.  
917 (Eds). Economic Geology 100<sup>th</sup> Anniversary Volume. Society of Economic Geologists,  
918 p523-560.

919 Friedrich, A.M., Bowring, S., Martin, M.W. & Hodges, K.V., 1999a, Short-lived continental  
920 magmatic arc at Connemara, western Irish Caledonides: Implications for the age of the  
921 Grampian orogeny. *Geology*, **27**, 27-30.

922 Friedrich, A.M., Hodges, K.V., Bowring, S. & Martin, M.W., 1999b, Geochronological  
923 constraints on the magmatic, metamorphic and thermal evolution of the Connemara  
924 Caledonides, western Ireland. *Journal of the Geological Society, London*, **156**, 1217-1230.

925 Fujisaki, W., Asanuma, H., Suzuki, K., Sawaki, Y., Sakata, S., Hirata, T., Maruyama, S. &  
926 Windley, B.F., 2015, Ordovician ocean plate stratigraphy and thrust duplexes of the  
927 Ballantrae Complex, SW Scotland: implications for pelagic deposition rate and forearc  
928 accretion in the closing Iapetus Ocean. *Tectonophysics*. Online First – DOI:  
929 10.1016/j.tecto.2015.04.2014

930 Hamilton, P.J., O’Nions, R.K., Bridgwater, D. & Nutman, A., 1983, Sm-Nd studies of  
931 Archaean metasediments and metavolcanics from West Greenland and their implications  
932 for the Earth’s early history. *Earth and Planetary Science Letters*, **62**, 263-272.

933 Herrington, R.J. & Brown, D., 2011, The generation and preservation of mineral deposits in  
934 arc-continent collision environments. In: Brown, D. & Ryan, P.D. (eds), *Arc-Continent*  
935 *Collision*. Frontiers in Earth Sciences. Springer-Verlag, Berlin Heidelberg. 145-159.

936 Herrington, R., Maslennikov, V., Zaykov, V., Seravkin, I., Kosarev, A., Buschmann, B.,  
937 Orgeval, J-J., Holland, N., Tesalina, S., Nimis, P. & Armstrong, R., 2005, 6: Classification  
938 of VMS deposits: Lessons from the South Uralides. *Ore Geology Reviews*, **27**, 203-237.

939 Herrington, R., Plotinskaya, O.Y., Maslennikov, V.V. & Tessalina, S.G., 2017. An overview  
940 of mineral deposits in the Urals: a special issue of Ore Geology Reviews. Ore Geology  
941 Reviews. DOI: 10.1016/j.oregeorev.2016.12.016

942 Hodgson, J.A. & Ture, M.D. 2014. Tellus Border Project; Airborne geophysical interpretation  
943 report. Geological Survey of Ireland and Geological Survey of Northern Ireland, 118 pages.  
944 [http://www.tellusborder.eu/NR/rdonlyres/1D774DD2-E14D-421A-95AB-](http://www.tellusborder.eu/NR/rdonlyres/1D774DD2-E14D-421A-95AB-0ADC60CD6C1C/0/TBGPH07%20Interpretation%20Report%2027June%202014.pdf)  
945 [0ADC60CD6C1C/0/TBGPH07 Interpretation Report 27June 2014.pdf](http://www.tellusborder.eu/NR/rdonlyres/1D774DD2-E14D-421A-95AB-0ADC60CD6C1C/0/TBGPH07%20Interpretation%20Report%2027June%202014.pdf)

946 Hollis, S.P., Roberts, S., Cooper, M.R., Earls, G., Herrington, R.J., Condon, D.J., Cooper, M.J.,  
947 Archibald, S.M. & Piercey, S.J., 2012. Episodic-arc ophiolite emplacement and the growth  
948 of continental margins: Late accretion in the Northern Irish sector of the Grampian-Taconic  
949 orogeny. *GSA Bulletin*, **124**, 1702-1723.

950 Hollis SP, Cooper MR, Roberts S, Herrington RJ, Earls G, & Condon, D.J., 2013a.  
951 Stratigraphic, geochemical and U-Pb zircon age constraints from Slieve Gallion, Northern  
952 Ireland: A correlation of the Irish Caledonian arcs. *Journal of the Geological Society,*  
953 *London*, **170**, 737-752.

954 Hollis S.P., Cooper M.R., Roberts S., Earls G., Herrington R.J., Condon D.J. & Daly, J.S.,  
955 2013b. Late obduction of the Tyrone ophiolite, Northern Ireland, during the Grampian-  
956 Taconic orogeny: a correlative of the Annieopsquotch ophiolite of Newfoundland? *Journal*  
957 *of the Geological Society, London*, **170**, 861-876.

958 Hollis, S.P., Roberts, S., Earls, G., Herrington, R., Cooper, M.R., Piercey S.J., Archibald, S.M.,  
959 & Moloney, M., 2014. Petrochemistry and hydrothermal alteration within the Tyrone  
960 Igneous Complex, Northern Ireland: implications for VMS mineralization in the peri-  
961 Laurentian British and Irish Caledonides. *Mineralium Deposita*, **49**, 575-593.

962 Hollis, S.P., Cooper, M.R., Herrington, R.J., Roberts, S., Earls, G., Verbeeten, A., Piercey, S.J.,  
963 & Archibald, S.M., 2015, Distribution, mineralogy and geochemistry of silica-iron exhalites  
964 and related rocks from the Tyrone Igneous Complex: implications for VMS mineralization  
965 in Northern Ireland. *Journal of Geochemical Exploration*, **159**, 148-168.

966 Hollis, S.P., Cooper, M.R., Earls, G., Roberts, S., Herrington, R.J. & Piercey, S.J. (2016).  
967 Using Tellus data to enhance targeting of volcanogenic massive sulphide mineralization in  
968 the Tyrone Igneous Complex. In: Young, M.E. (ed.) *Unearthed: impacts of the Tellus*  
969 *surveys of the north of Ireland*. Dublin. Royal Irish Academy, p157-168.

970 Hutton, D.H.W., Aftalion, M. & Halliday, A.N., 1985, An Ordovician ophiolite in County  
971 Tyrone, Ireland. *Nature*, **315**, 310-312.

972 Jeffries, T.E., Fernández-Suárez, J., Corfu, F. & Alonso, G.G., 2003, Advances in U-Pb  
973 geochronology using frequency quintupled Nd:YAG based laser ablation system ( $\lambda =$   
974 213nm) and quadrupole based ICP-MS. *Journal of Analytical Atomic Spectrometry*, **18**,  
975 847-855.

976 Kerrich, R., Goldfarb, R.J. & Richards, J.P., 2005, Metallogenic provinces in an evolving  
977 geodynamic framework. Society of Economic Geologists, Inc., Econ. Geol. 100th  
978 Anniversary Vol., 1097–1136.

979 Landing, E., Rushton, A.W.A., Fortey, R.A. & Bowring, S.A., 2005, Improved geochronologic  
980 accuracy and precision for the ICS chronostratigraphic charts: examples from the late  
981 Cambrian – Early Ordovician. *Episodes*, **38**, 154-161.

982 Large, R.R., Gemmell, J.B. & Paulick, H., 2001, The alteration box plot: a simple approach to  
983 understanding the relationship between alteration mineralogy and litho geochemistry  
984 associated with volcanic-hosted massive sulfide deposits. *Economic Geology*, **96**, 957-971.

985 Leshner, C.M., Goodwin, A.M., Campbell, I.H. & Gorton, M.P., 1986, Trace-element  
986 geochemistry of ore-associated and barren, felsic metavolcanic rocks in the Superior  
987 province, Canada. *Canadian Journal of Earth Sciences*, **23**, 222-237.

988 Lindskog, A., Costa, M.M., Rasmussen, C.M.Ø., Conneally, J.N. & Eriksson, M.E., 2016.  
989 Refined Ordovician timescale reveals no link between asteroid breakup and  
990 biodiversification. *Nature Communications*. DOI: 10.1038/ncomms14066

991 Long, C. B., McConnell, B.J., & Philcox, M.E., 2005. Geology of South Mayo: a Geological  
992 Description, with accompanying Bedrock Geology 1:100,000 Scale Map, Sheet 11, South  
993 Mayo. Geological Survey of Ireland, Dublin.

994 Lowell, J.D. & Guilbert, J.M., 1970, Lateral and vertical alteration-mineralization zoning in  
995 porphyry ore deposits. *Economic Geology*, **65**, 373-408.

996 Ludwig, K.R., 2001, Isoplot/Ex, rev. 2.49. A Geochronological Toolkit for Microsoft Excel:  
997 Berkeley Geochronology Center, Special Publication No. 1a.

998 MacLean, W.H., 1990, Mass change calculation in altered rock series. *Mineralium Deposita*,  
999 **23**, 231-238.

1000 McLean, N.M., Condon, D.J., Schoene, B. & Bowring, S.A., 2015, Evaluating uncertainties in  
1001 the calibration of isotopic reference materials and multi-element isotopic tracers  
1002 (EARTHTIME Tracer Calibration Part II). *Geochimica et Cosmochimica Acta*, **164**, 481–  
1003 501



- 1004 Mattinson, J.M., 2005. Zircon U–Pb chemical abrasion ('CA-TIMS') method: Combined  
1005 annealing and multi-step partial dissolution analysis for improved precision and accuracy of  
1006 zircon ages. *Chemical Geology* 220, 47–66. doi:10.1016/j.chemgeo.2005.03.011
- 1007 McConnell, B., Crowley, Q.G. & Riggs, N., 2010, Laurentian origin of the Ordovician  
1008 Grangegeeth volcanic arc terrane, Ireland. *Journal of the Geological Society, London*, **167**,  
1009 469-474.
- 1010 McConnell, B., Riggs, N. & Crowley, Q.G., 2009, Detrital zircon provenance and Ordovician  
1011 terrane amalgamation, western Ireland. *Journal of the Geological Society, London*, **166**,  
1012 **473-484**.
- 1013 McDonough, W.F. & Sun S-S., 1995, The composition of the Earth. *Chemical Geology*, **120**,  
1014 223-254
- 1015 O'Connor, P.G., 1987, Volcanology, geochemistry and mineralization in the Charlestown  
1016 Ordovician inlier, Co. Mayo. PhD thesis, University College Dublin, Ireland.
- 1017 O'Connor, P.G. & Poustie, A., 1986, Geological setting of, and alteration associated with, the  
1018 Charlestown mineral deposit. *In: Andrew, C.J., Crowe, R.W.A., Finley, F., Pennell, W.M.,*  
1019 *& Pyne, J.F.L. (eds). The Geology and Genesis of Mineral Deposits in Ireland.* Irish  
1020 Association of Economic Geology, 89-102.
- 1021 Oliver, G.J.H., Chen, F., Buchwaldt, R. & Hegner, E., 2000, Fast tectonometamorphism and  
1022 exhumation in the type area of the Barrovian and Buchan zones. *Geology*, **28**, 459-462.
- 1023 Oliver, G.J.H., Wilde, S. & Wan, Y., 2008, Geochronology and geodynamics of Scottish  
1024 granitoids from the late Neoproterozoic break-up of Rodinia to Palaeozoic collision. *Journal*  
1025 *of the Geological Society, London*, **165**, 661-674.
- 1026 Parnell, J., Earls, G., Wilkinson, J.J., Hutton, D.H.W., Boyce, A.J., Fallick, A.E., Ellam, R.M.,  
1027 2000, Regional fluid flow and gold mineralization in the Dalradian of the Sperrin  
1028 Mountains, Northern Ireland. *Economic Geology*, **95**, 1389-1416.
- 1029 Pearce, J.A., 1996, A user's guide to basalt discrimination diagrams. *In: Wyman, D.A. (ed.)*,  
1030 *Trace element geochemistry of volcanic rocks: applications for massive-sulphide*  
1031 *exploration.* Geological Association of Canada, Short Course Notes 12, 79-113.
- 1032 Pearce, J.A., 2008, Geochemical fingerprinting of oceanic basalts with applications to ophiolite  
1033 classification and the search for Archean oceanic crust. *Lithos*, **100**, 14-48.
- 1034 Pearce, J.A. & Cann, J.R., 1973, Tectonic setting of basic volcanic rocks determined using  
1035 trace element analyses. *Earth and Planetary Science Letters*, **19**, 290-300.
- 1036 Pearce, J.A., Harris, N.B.W. & Tindle, A.G., 1984, Trace element discrimination diagrams for  
1037 the tectonic interpretation of granitic rocks. *Journal of Petrology*, **25**, 956-983.

1038 Peatfield, G.R., 2003, Updated technical review report on the Tyrone mineral exploration  
1039 property, (prospecting licences UM 11/96 and UM 12/96, County Tyrone, Northern Ireland  
1040 – 20 January, 2003. Published report for Tournigan Gold Corporation

1041 Poustie, A., 1982, The discovery of a new mineral deposit within an Ordovician volcanic series  
1042 near Charlestown, Co. Mayo. *In: Brown, A.G. (ed.), Mineral Exploration in Ireland:  
1043 Progress and Developments 1971-1981.* Irish Association for Economic Geology.

1044 Piercey, S.J., 2007, Volcanogenic massive sulphide (VMS) deposits of the Newfoundland  
1045 Appalachians: An overview of their setting, classification, grade-tonnage data, and  
1046 unresolved questions. *In Pereira, C.G.P. & Walsh, D.G. (eds) Current Research.*  
1047 Newfoundland Department of Natural Resources, Geological Survey, Report 07-01: pp 169-  
1048 178

1049 Piercey, S.J., 2011, The setting, style, and role of magmatism in the formation of volcanogenic  
1050 massive sulfide deposits. *Mineralium Deposita*, **46**, 449-471

1051 Reynolds, G., 2014, Charlestown – the copper mine that got away. *Earth Science Ireland*, **15**,  
1052 37-38.

1053 Rice, C. M., Mark, D. F., Selby, D. & Neilson, J.E., & Davidheiser-Kroll, B. 2016, Age and  
1054 geologic setting of quartz vein-hosted gold mineralization at Curraghinalt, Northern Ireland:  
1055 implications for genesis and classification. *Economic Geology*, **111**, 127-150.

1056 Rogers, N., van Staal, C.R., Zagorevshki, I., Skulski, T., Piercey, S. & McNicoll, V.J., 2007,  
1057 Timing and tectonic setting of volcanogenic massive sulphide bearing terranes within the  
1058 Central Mobile Belt of the Canadian Appalachians. *In: Milkereit, B. (ed.) Exploration in the  
1059 New Millennium, Proceedings of the Fifth Decennial International Conference on Mineral  
1060 Exploration.* Decennial Mineral Exploration Conferences, Toronto, Canada, 1199–1205.

1061 Ross, P.-S. & Bédard, J.H., 2009, Magmatic affinity of modern and ancient subalkaline  
1062 volcanic rocks determined from trace-element discrimination diagrams. *Canadian Journal  
1063 of Earth Science*, **46**, 823-839.

1064 Rushton, A.W.A., 2014, A Yapeenian (Late Arenig) graptolite fauna from the Ordovician rocks  
1065 of the Charlestown Inlier, Co. Mayo, Ireland. *Irish Journal of Earth Sciences*, **32**, 79-87.

1066 Ryan, P.D. & Dewey, J.F., 2011, Arc-continent collision in the Ordovician of western Ireland:  
1067 stratigraphic, structural and metamorphic evolution. *In: Brown, D. & Ryan, P.D., (eds.).  
1068 Arc-Continent Collision.* Frontiers in Earth Sciences. Springer-Verlag Belin Heidelberg,  
1069 373-401.

- 1070 Ryan, P.D., Floyd, P.A. & Archer, J.B., 1980, The stratigraphy and petrochemistry of the  
1071 Lough Nafooy Group (Tremadocian), western Ireland. *Journal of the Geological Society,*  
1072 *London*, **137**, 443-458.
- 1073 Sadler, P.M., Cooper, R.A. & Melchin, M., 2009, High-resolution, early Paleozoic  
1074 (Ordovician-Silurian) time scales. *GSA Bulletin*, **121**, 887-906.
- 1075 Schandl, E.S. & Gorton, M.P., 2002, Application of high field strength elements to discriminate  
1076 tectonic settings in VMS environments. *Economic Geology*, **97**, 629-642.
- 1077 Schmitz, M.D., 2012, Appendix 2 – Radiometric ages used in GTS2012. In: Gradstein, F.M.,  
1078 Ogg, J.G., Schmitz, M. & Ogg, G. (eds.) *The Geologic Time Scale 2012*. Elsevier B.V.  
1079 Pages 1045-1082.
- 1080 Spray, J.G. & Dunning, G.R., 1991, A U/Pb age for the Shetland Island oceanic fragment,  
1081 Scottish Caledonides: evidence from anatectic plagiogranites in ‘layer 3’ shear zones.  
1082 *Geological Magazine*, **128**, 667-671.
- 1083 Stobbs, I., 2013, *The Charlestown Inlier, Co. Mayo: mineralisation, geochemistry and regional*  
1084 *correlation with allochthonous Caledonian island arcs across Ireland*. MSci thesis, Imperial  
1085 College London, 61pp.
- 1086 Stone, P., 2014, A review of geological origins and relationships in the Ballantrae Complex,  
1087 SW Scotland. *Scottish Journal of Geology*, **50**, 1-25.
- 1088 Tapster, S., Condon, D.J., Naden, J., Noble, S.R., Petterson, M.G., Roberts, N.M.W., Saunders,  
1089 A.D. & Smith, D.J., 2016. Rapid thermal rejuvenation of high-crystallinity magma linked  
1090 to porphyry copper deposit formation; evidence from the Koloula Porphyry Prospect,  
1091 Solomon Islands. *Earth and Planetary Science Letters*, **442**, 206-217.
- 1092 Thirlwall, M.F. & Bluck, B.J., 1984, Sr–Nd isotope and geological evidence that the Ballantrae  
1093 “ophiolite”, SW Scotland, is polygenetic. In: Gass, I.G., Lippard, S.J., Shelton, A.W. (eds.),  
1094 *Ophiolites and Oceanic Lithosphere*. Journal of the Geological Society, London, Special  
1095 Publication 13, 215–230.
- 1096 van Staal, C.R., 2007, Pre-Carboniferous tectonic evolution and metallogeny of the Canadian  
1097 Appalachians. In Goodfellow, W.D. (ed) *Mineral Deposits of Canada: A synthesis of major*  
1098 *deposit-types, district metallogeny, the evolution of geological provinces, and exploration*  
1099 *methods*. Geological Association of Canada, Mineral Deposits Division, Special Publication  
1100 5, 793-818
- 1101 van staal, C.R., Chew, D.M., Zagorevski, A., McNicoll, V., Hibbard, J., Skulski, T.,  
1102 Castonguay, S., Escayola, M.P., Sylvester, P.J., 2014, Evidence of Late Ediacaran  
1103 hyperextension of the Laurentian Iapetan margin in the Birchy Complex, Baie Verte

1104 Peninsula, northwest Newfoundland: implications for the Opening of Iapetus, Formation of  
1105 peri-Laurentian microcontinents and Taconic-Grampian orogenesis. *Geoscience Canada*,  
1106 **40**, <http://dx.doi.org/10.12789/geocanj.2013.40.006>.

1107 Wiedenbeck, M., Allé, P., Corfu, F., Griffin, W. L., Meier, M., Oberli, F., von Quadt, A.,  
1108 Roddick, J. C. & Spiegel, W., 1995, Three natural zircon standards for U-Th-Pb, Lu-Hf,  
1109 trace element and REE analysis: *Geostandards Newsletter*, v. 19, p. 1- 23.

1110 Wood, D.A., 1980, The application of a Th-Hf-Ta diagram to problems of tectonomagmatic  
1111 classification and to establishing the nature of crustal contamination of basaltic lavas of the  
1112 British Tertiary Volcanic Province. *Earth and Planetary Science Letters*, **50**, 11-30.

1113 Wrafter, J.P. & Graham, J.R., 1989, Ophiolitic detritus in the Ordovician sediments of  
1114 South Mayo, Ireland. *Journal of the Geological Society, London*, **146**, 213–215.

1115 Yeats, C.J., Hollis, S.P., Halfpenny, A., Corona, J-C., LaFlamme, C., Southam, G., Fiorentini,  
1116 M., Herrington, R.J. & Spratt, J., 2017, Actively forming Kuroko-type volcanic-hosted  
1117 massive sulfide (VHMS) mineralization at Iheya North, Okinawa Trough, Japan. *Ore*  
1118 *Geology Reviews*, **84**, 20-41.

1119 Young, M.E. & Donald, A.W., 2013, A guide to the Tellus data. Geological Survey of Northern  
1120 Ireland, Belfast, p233.

1121

1122 **Figure Captions:**

1123 **Fig. 1. (a)** Setting of the Charlestown Group and other comparable ophiolite and volcanic arc  
1124 associations in Britain and Ireland. **(b)** Simplified regional geology of Newfoundland. **(c)** Early  
1125 Mesozoic restoration of North Atlantic region and Appalachian-Caledonian orogen. Figure  
1126 after Cooper et al. (2011).

1127

1128 **Fig. 2.** Cartoon detailing the tectonic evolution of the northern British and Irish Caledonides  
1129 during the Grampian event, based on the three equivalent and well-documented arc/ophiolite  
1130 accretion events recognized in the Newfoundland Appalachians (modified after van Staal et al.  
1131 2007; 2014; Chew et al. 2010; Hollis et al. 2012). **(a)** Early formation of the suprasubduction  
1132 affinity Deer Park (DP;  $>514 \pm 3$  Ma) and Highland Border (HB;  $499 \pm 8$  Ma) ophiolites (Chew  
1133 et al., 2010) between the Laurentian margin and outriding microcontinental blocks (such as the  
1134 Sliswood Division, Tyrone Central Inlier and Midland Valley block). **(b)** Continued closure  
1135 of the Iapetus Ocean and clogging of the subduction channel led to ophiolite obduction at c.  
1136 490 Ma, and subduction polarity reversal. Metamorphism and obduction of the HB ophiolite is  
1137 constrained by  $^{40}\text{Ar}$ - $^{39}\text{Ar}$  ages of  $490 \pm 4$  Ma (hornblende) and  $488 \pm 1$  Ma (muscovite) (Chew

1138 et al., 2010). The juvenile Lough Nafooeey arc system developed above a south-dipping  
1139 subduction zone from c. 490 Ma (Draut et al., 2004), with its fore-arc preserved as the South  
1140 Mayo Trough (SMT), and accretionary prism preserved as the Clew Bay Complex (CBC). The  
1141 Shetland/Unst ophiolite formed at this time (c.  $492 \pm 3$  Ma: Spray and Dunning, 1991), most  
1142 likely as an oceanic core complex (see Crowley and Strachan, 2014; not shown) along strike  
1143 from the Lough Nafooeey arc system. **(c)** Hard arc-continent collision between the Lough  
1144 Nafooeey arc and the Laurentian margin occurred between c. 484 and 478 Ma (Draut et al.,  
1145 2004; **Fig. 11**), resulting in the exhumation of the DP ophiolite at  $482 \pm 1$  Ma (Chew et al.,  
1146 2010), with ophiolitic detritus recorded in the younger Letterbrock Formation of the SMT  
1147 (Wrafter and Graham, 1989, Dewey and Mange, 1999; **Fig. 11**). The obduction of the Shetland  
1148 ophiolite also occurred around this time ( $484 \pm 4$  Ma; Crowley and Strachan, 2014; not shown).  
1149 Hard arc-continent collision at was associated with syncollisional volcanism in the  
1150 Tourmakeady Group, and led to the initiation of north-dipping subduction outboard of the  
1151 composite Laurentian margin and the formation of the late c. 484-479 Ma suprasubduction  
1152 affinity ophiolites (i.e. Tyrone and Ballantrae; Hollis et al., 2013a; Stone, 2014). Both the  
1153 Ballantrae and Tyrone ophiolites may have been obducted shortly after their formation as  
1154 collisional thickening progressed SE. Rapid obduction is indicated by K-Ar ages from the  
1155 metamorphic sole of the Ballantrae ophiolite (c.  $478 \pm 9$  Ma; Bluck et al., 1980) and the  
1156 recognition of S-type granites in Co. Tyrone constrained to c. 479 Ma (Hollis et al.,  
1157 unpublished). **(d)** Peak deformation and metamorphism was reached in the Grampian event  
1158 between c. 475 and 465 Ma (reviewed in Chew, 2009). The Tyrone and Ballantrae arc volcanics  
1159 most likely developed outboard of the composite margin (from c. 475 Ma; **Fig. 11**), as they  
1160 show evidence for extensive arc-rifting, with arc-obduction in Tyrone occurring prior to c. 470  
1161 Ma (Hollis et al., 2013a). Continued northward subduction led to the development of the  
1162 Southern Uplands (SU) – Down Longford (DL) Terrane, a Late Ordovician to Silurian  
1163 accretionary prism.

1164

1165

1166 **Fig. 3. (a)** Geological map of Charlestown Inlier (after Long et al., 2005). White crosses A to  
1167 C denote graptolite localities (A and B from Cummins, 1954; C new Knock Airport fauna). C  
1168 also denotes the position of samples for CA-ID-TIMS U-Pb zircon geochronology. **(b)**  
1169 Geological line work of the Charlestown Group (from **Fig. 3a**) superimposed over the Tellus  
1170 Border (Hodgson and Ture, 2014) Total Magnetic Intensity map highlighting the extension of  
1171 the Charlestown Group under Carboniferous cover for at least 4km to the NE and 10km to the

1172 SW. Two 2km x 4km circular magnetic features to the east of the Charlestown Inlier most  
1173 likely represent concealed Late Caledonian intrusions.

1174

1175 **Fig. 4.** Cross section through the Charlestown Cu deposit (modified after O'Connor and  
1176 Poustie, 1986). Type 1 and 2 breccias developed around the upper margins of the QFP units as  
1177 magma was intruded into unconsolidated wet sediment (forming peperitic contacts) just below  
1178 the seafloor. Chalcopyrite mineralization occurred directly below, and within, the zone of  
1179 pyrite mineralization, above the chloritic feeder zone. Sphalerite mineralization occurs down-  
1180 dip of the pyrite zone, precipitating from cooler hydrothermal fluids during seawater  
1181 entrainment into the brecciated QPF margin. The barite zone of O'Connor and Poustie (1986)  
1182 is not shown, but overlaps the area of pyrite and chalcopyrite mineralization. Chloritic-sericitic  
1183 alteration occurs in the hanging-wall and flanks of the deposit. A silicified central zone is also  
1184 consistent with a VMS system.

1185

1186 **Fig. 5. (a)** Knock Airport logged section showing the position of samples collected for  
1187 biostratigraphy and U-Pb zircon dating. **(b)** Banded crystal tuff (KGC2). **(c)** Graptolite bearing  
1188 mudstone which yielded the Ya2 fauna described in Rushton (2014). **(d)** Contact between  
1189 pyroxene diorite and laminated mudstones.

1190

1191

1192 **Fig. 6.** Scanning Electron Microscope (SEM) images of alteration assemblages throughout the  
1193 Charlestown Group. (a) CT113: Crystal tuff from the Horan Formation. (b) CT206: Altered  
1194 felsic volcanic breccia from the Carracastle Formation.

1195

1196 **Fig. 7.** Selected graptolite fauna identified from the Charlestown Group. **(a)** *Pseudisograptus*  
1197 *manubriatus* (Hall) group, Natural History Museum QQ.265. Knock Airport section. **(b)**  
1198 *Yutagraptus? v-deflexus* (Harris), Natural History Museum QQ.262. Knock Airport section.  
1199 **(c)** *Didymograptus (Expansograptus) aff. nitidus* (J. Hall), Sedgwick Museum A.61368.  
1200 Cummins' locality A. **(d)** *Isograptus caduceus? cf. nanus* Ruedemann, Natural History  
1201 Museum QQ.263b, partly restored from the counterpart, QQ.263a. Knock Airport section. **(e)**  
1202 *Arienigraptus? sp.*, Natural History Museum QQ.264. Knock Airport section. **(f)** *Oncograptus*  
1203 *sp.*, Sedgwick Museum A.24401. Cummins' locality A. **(g-i)** *Exigraptus uniformis* Mu, Natural  
1204 History Museum, QQ.277, QQ.275 and QQ.274a. Graptolite shown in g is a juvenile specimen.

1205 Knock Airport section. **(j-k)** *Skiagraptus gnomonicus* (Harris and Keble), Natural History  
1206 Museum QQ.269 and QQ.270. Knock Airport section. All scale bars are 2mm in length.

1207

1208 **Fig. 8.** U-Pb zircon ages for the four dated samples from the Horan Formation of the  
1209 Charlestown Group.

1210

1211 **Fig. 9.** Geochemical variation of the Charlestown Group. **(a)** Zr/Ti vs. Nb/Y discrimination  
1212 diagram for the classification of hydrothermally altered volcanic rocks after Pearce (1996).  
1213 Ellipses represent 10% probability contours (that is 10% of the samples from that group will  
1214 plot outside the respective contour) to highlight potential misidentifications using the diagram.  
1215 **(b)** Nb vs. Y discrimination diagram for the classification of felsic rocks after Pearce et al.  
1216 (1984; ORG, orogenic granite; synCOLG, syncollisional granite; VAG, volcanic arc granite;  
1217 WPG, within-plate granitic). **(c)** Zr/Y vs. Y diagram for the classification of VMS fertile felsic  
1218 rocks after Lesher et al. (1986). Samples which plot in the FIII fields are considered the most  
1219 prospective for Phanerozoic arcs. **(d)** Nb/Y vs Zr/Y diagram highlighting the geochemical  
1220 affinity of samples from Charlestown (tholeiitic to calc-alkaline) and similarities to the Tyrone  
1221 Volcanic Group of Northern Ireland (data compiled from Draut et al., 2009; Cooper et al.,  
1222 2011; Hollis, 2013; Hollis et al. 2012, 2013b; 2014). **(e)** Th/Yb vs. Nb/Yb diagram of Pearce  
1223 (2008). Samples from the Charlestown Group plot on a trend parallel to the mantle array  
1224 indicating a subduction affinity for the lavas. **(f)** La-Nb-Y ternary discrimination diagram for  
1225 the classification of mafic volcanic rocks after Cabanis and Lecolle (1989). **(g)** Th-Zr-Nb  
1226 ternary discrimination diagram for the classification of mafic volcanic rocks after Wood (1980;  
1227 alk, alkaline basalt; CAB, calc-alkaline basalt; eMORB, enriched mid ocean ridge basalt;  
1228 nMORB, normal mid ocean ridge basalt; IAT, island arc tholeiitic basalt). **(h)** Alteration Box  
1229 Plot of major element mobility (after Large et al. 2001). Red arrows show 5 common trends  
1230 during hydrothermal alteration. *Alteration mineralogy*: carb, carbonate; chl, chlorite; kfeld, K-  
1231 feldspar; py, pyrite; ser, sericite.  $AI=100*[K_2O+MgO]/[K_2O+MgO+CaO+Na_2O]$ .  
1232  $CCPI=100*[Fe_2O_3T+MgO]/[Fe_2O_3T+MgO+K_2O+Na_2O]$ .

1233

1234 **Fig. 10.** Chondrite normalized extended REE diagrams for samples analyzed herein from the  
1235 Charlestown Group. Grey fields denote datasets from western Ireland (Draut et al., 2002, 2004)  
1236 and the Tyrone Igneous Complex (Draut et al., 2009; Cooper et al., 2011; Hollis, 2013; Hollis  
1237 et al. 2012, 2013b; 2014). Chondrite normalization values from McDonough and Sun (1995).

1238

1239 **Fig. 11.** Stratigraphy, geochemistry and absolute ages for the Ordovician successions of the  
1240 Irish Caledonides and western Scotland. Diagram modified after Ryan and Dewey (2011) and  
1241 Hollis et al. (2013a). The standard British Ordovician stages, those of the IUGS and the  
1242 Australian Ordovician graptolite zones are assigned to absolute ages after Sadler et al. (2009).  
1243 Absolute ages for events are represented by red stars with error bars. Stratigraphy of the Tyrone  
1244 Volcanic Group after Hollis et al. (2012, 2013a, 2014). North and south limbs refer to the  
1245 Mweelrea syncline (South Mayo Trough). References to biostratigraphic and U-Pb zircon  
1246 constraints are from Hollis et al. (2013a). Biostratigraphic and U-Pb zircon constraints from  
1247 the Ballantrae Ophiolite Complex are from the recent review of Stone (2014) and Fujisaki et  
1248 al. (2015). Correlations for sedimentary dominated successions are shown in greyscale. Red  
1249 horizontal bars mark the position of ignimbrites and tuffs.

1250

1251 **Fig. 12.** Timescale of the Middle Ordovician modified after Lindskog et al. (2016). Note that  
1252 both the GTS 2012 and Lindskog et al. (2016) timescales include the erroneous calibration  
1253 point from Formil (Cooper et al., 2008). Only on the Sadler et al. (2009) timescale, which does  
1254 not include the Formil age, do our new CA-ID-TIMS ages match the Ya2 graptolite constraints.

1255

1256 **Fig. 13.** Schematic cartoon showing the evolution of the Charlestown Cu deposit. A)   
1257 Emplacement of a subvolcanic intrusion into unconsolidated sediments and volcaniclastics. B)   
1258 Extrusion of quartz-feldspar phyric dacitic lava and the deposition of crystal tuffs, with   
1259 localized peperite development. Synvolcanic sills are also emplaced at shallow levels.   
1260 Hydrothermal circulation is developed through cold down-welling seawater, with heat   
1261 provided by the underlying magmatism. C) Iron-silica-oxyhydroxides are precipitated as a   
1262 jasper apron from seafloor exhalation. Mineralization develops where hydrothermal fluids are   
1263 focused towards the seafloor, with the separation of sphalerite, pyrite and chalcopyrite.   
1264 Underlying volcanic rocks are hydrothermally altered, with intense chloritization in the feeder   
1265 zone and more distal zones of quartz-sericite±chlorite alteration. D) Continued burial of the   
1266 system, with the development of sericitic-chloritic alteration in the hanging-wall of the   
1267 Charlestown Cu deposit.

1268

1269 **Table 1.** U-Pb zircon geochronology data for samples analyzed by CA-ID-TIMS from the   
1270 Charlestown Group.

1271



1272 **Table 2.** Graptolite fauna originally identified by Cummins (1954) and revised by Dewey et  
 1273 al. (1970) from the Charlestown Group.

1274

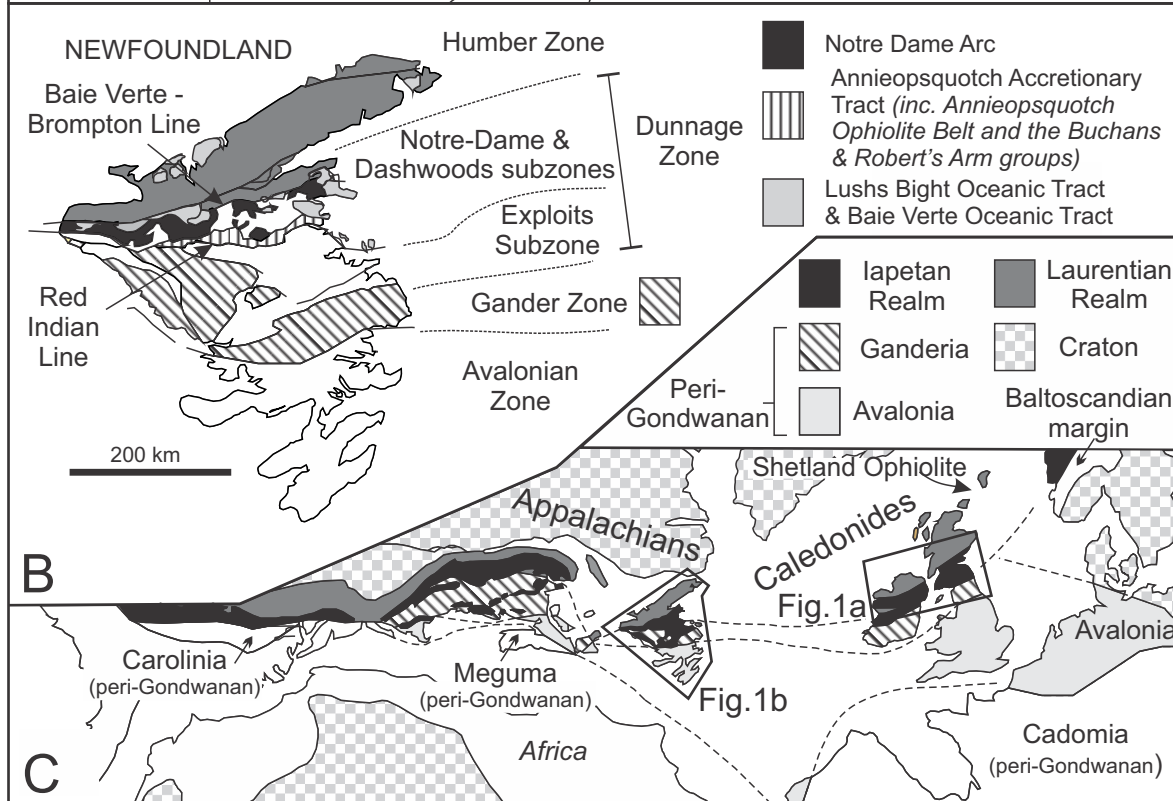
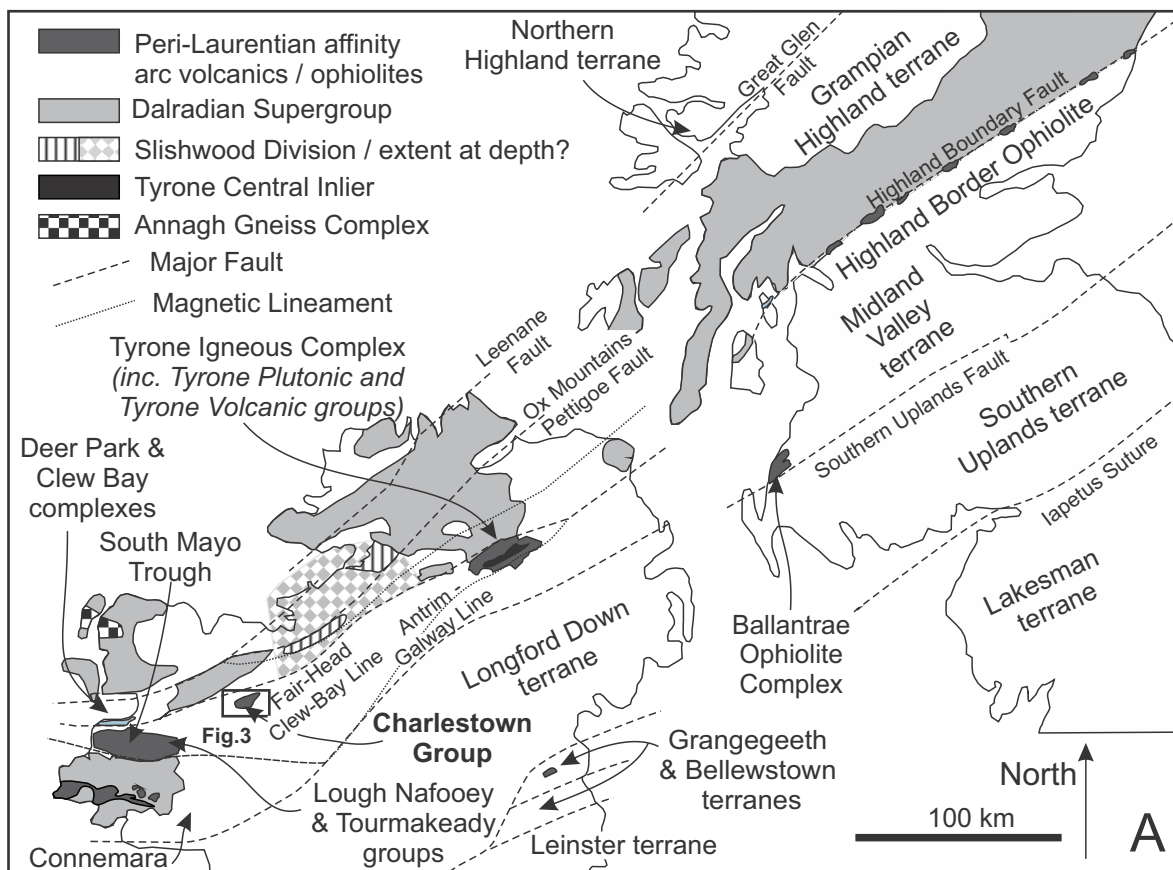
<b>Cummins (1954)</b>	<b>Dewey et al. (1970)</b>	
<i>Didymograptus</i> spp. (extensiform)	<i>D. cf. extensus</i> and <i>D. aff. nitidus</i>	<b>Fig. 7c</b>
<i>D. cf. deflexus</i> Elles & Wood	<i>D. cf. v-deflexus</i> Harris	
<i>Isograptus gibberulus</i> cf. <i>nanus</i> Ruedeman	<i>Oncograptus?</i> [juv.]	<b>Fig. 7f.</b>
<i>Glossograptus</i> sp.	? <i>G. crudus gisbornensis</i> Harris & Thomas	
<i>Oncograptus</i> sp.	? <i>O. upsilon biangulatus</i> Hall	
<i>Phyllograptus?</i> sp.	? <i>Trigonograptus ensiformis</i>	
<i>Tetragraptus</i> sp.		

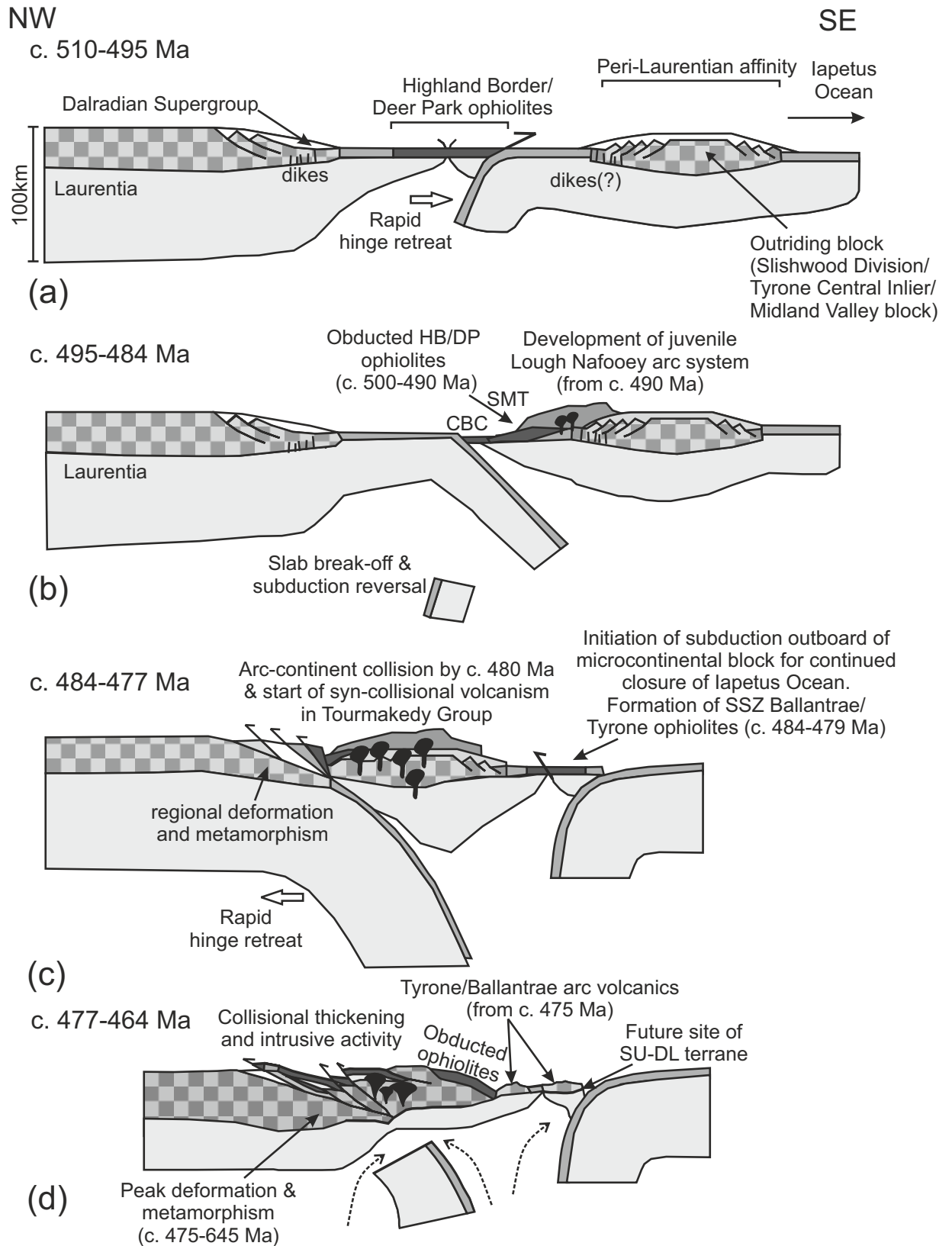
1275

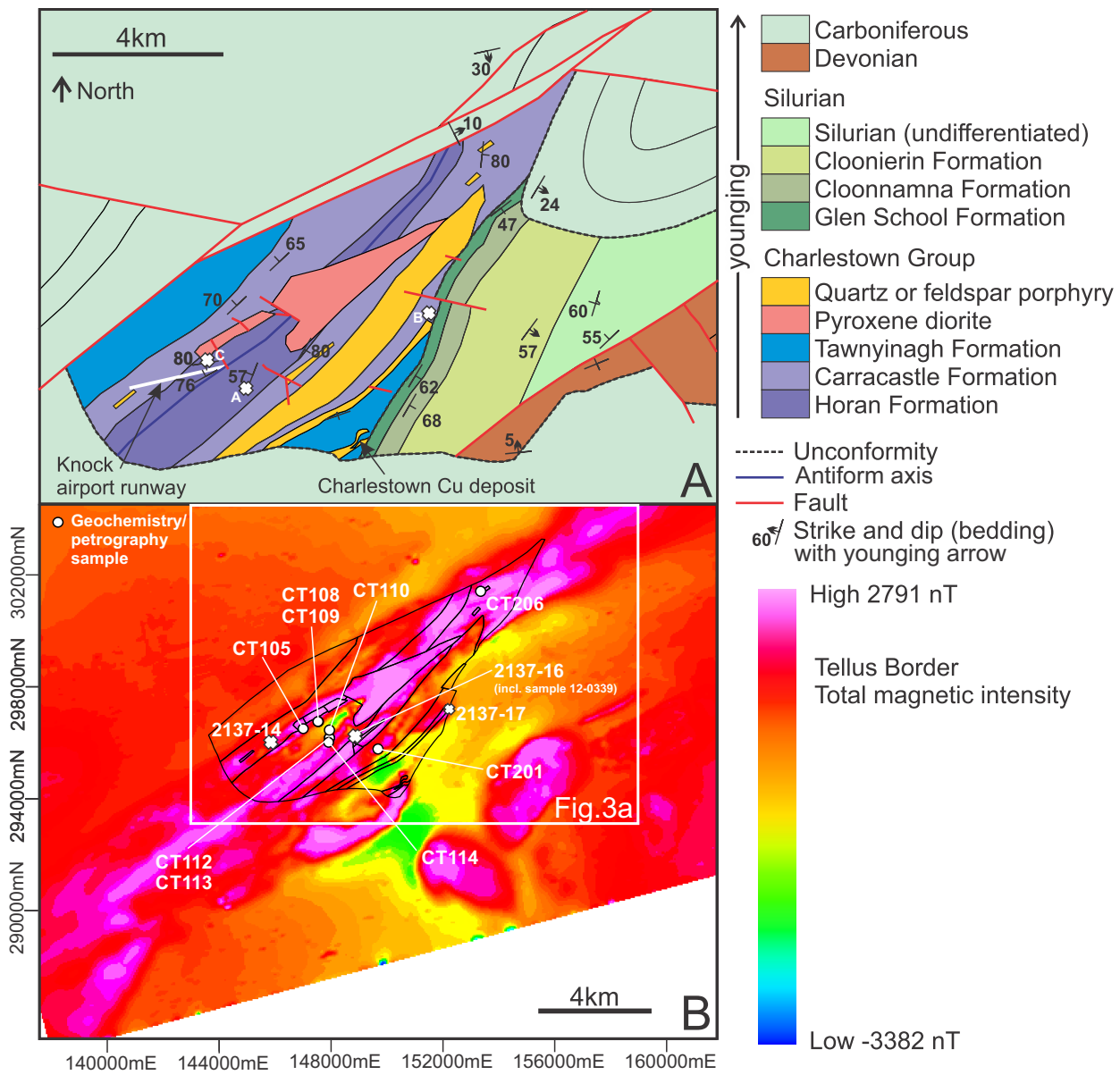
1276

1277 **Supplementary Information.** Whole rock geochemistry data from the Charlestown Group.

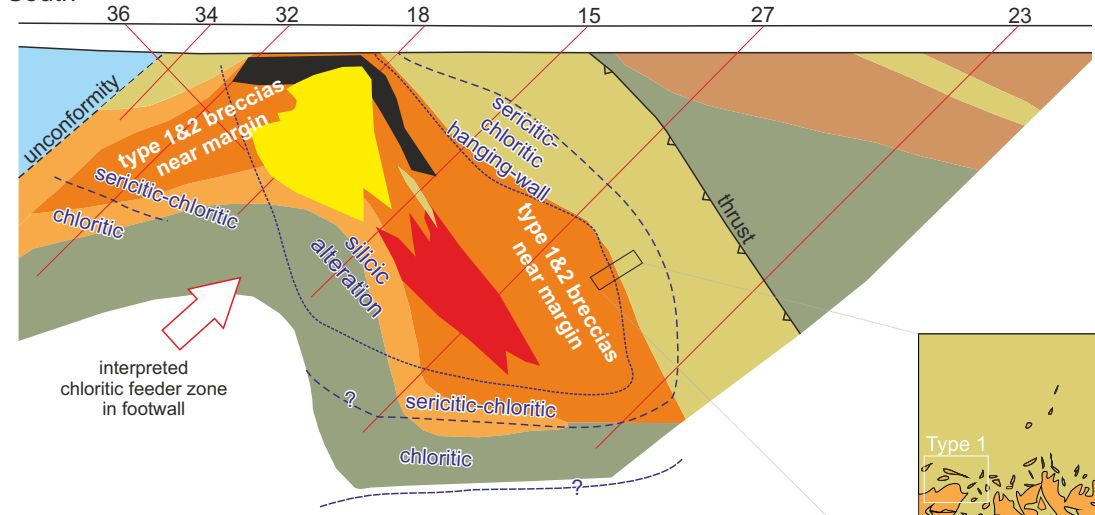
1278







South North

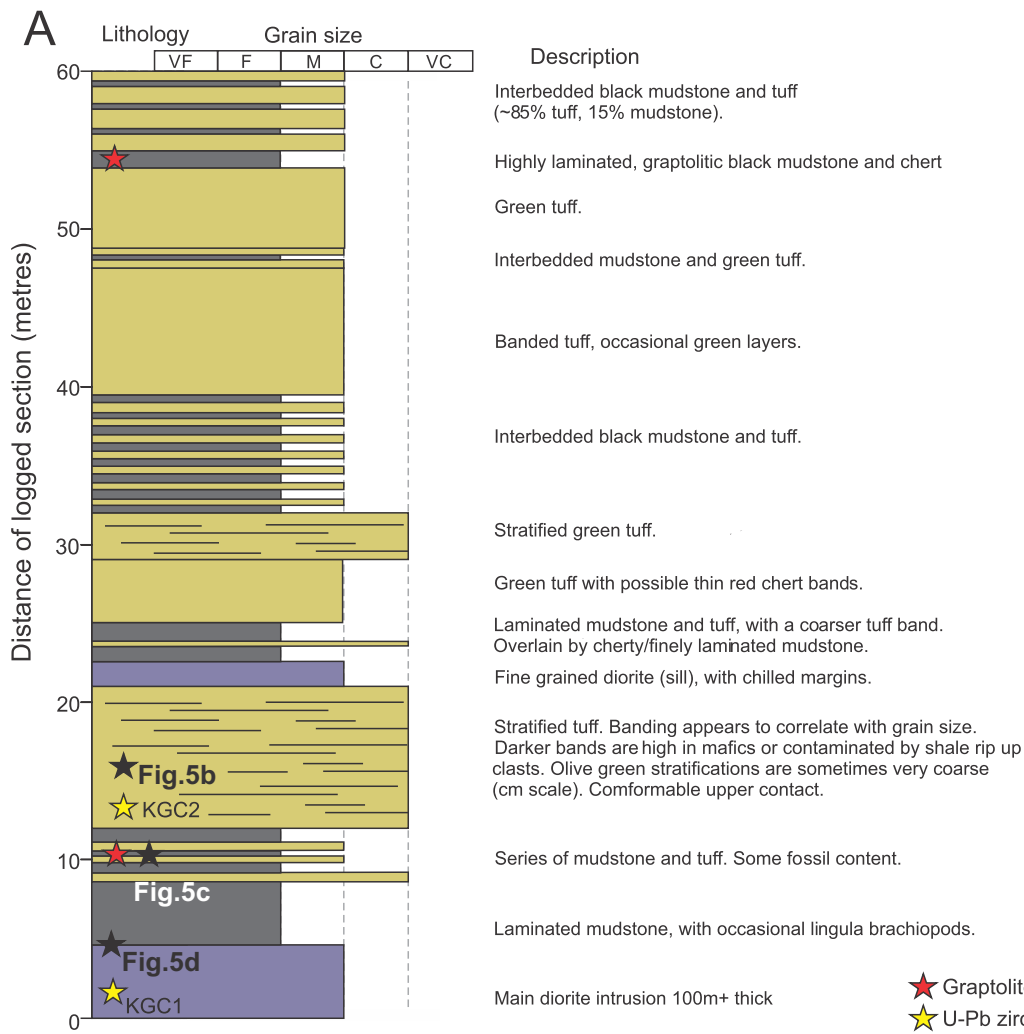


- Silurian (pebbly sandstone)
- Tuff (inc. ash, crystal, blocky & lapilli)
- Quartz-feldspar porphyry with xenoliths
- Quartz-feldspar porphyry
- Feldspar porphyry
- Andesite

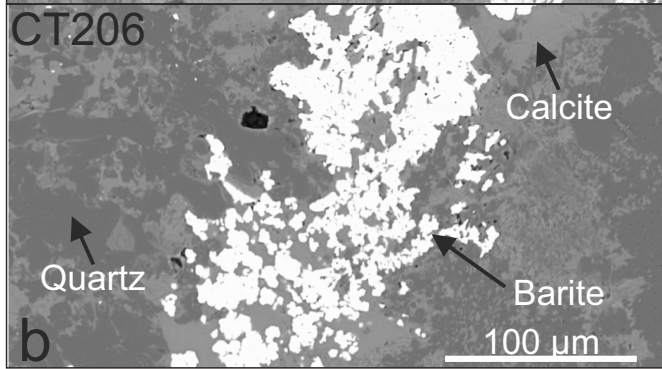
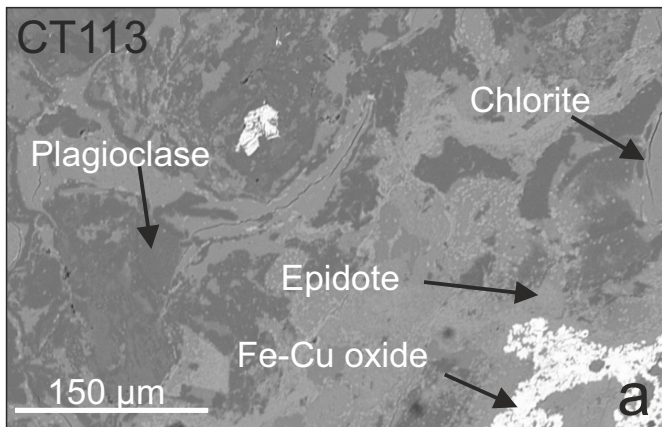
- Pyrite
- Sphalerite
- Chalcopyrite
- Silicic alteration
- Sericitic-chloritic alteration
- Chloritic alteration

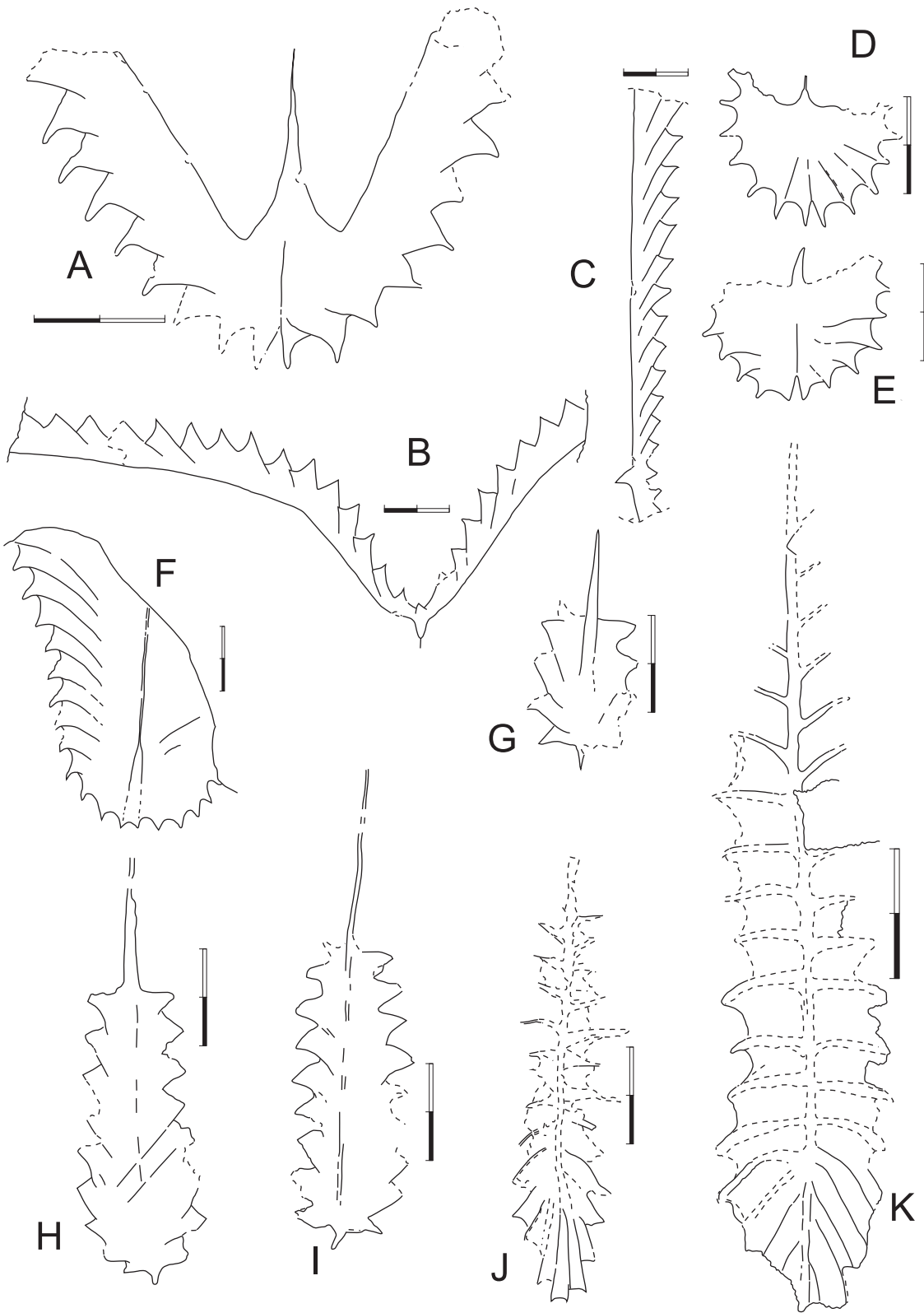


60m

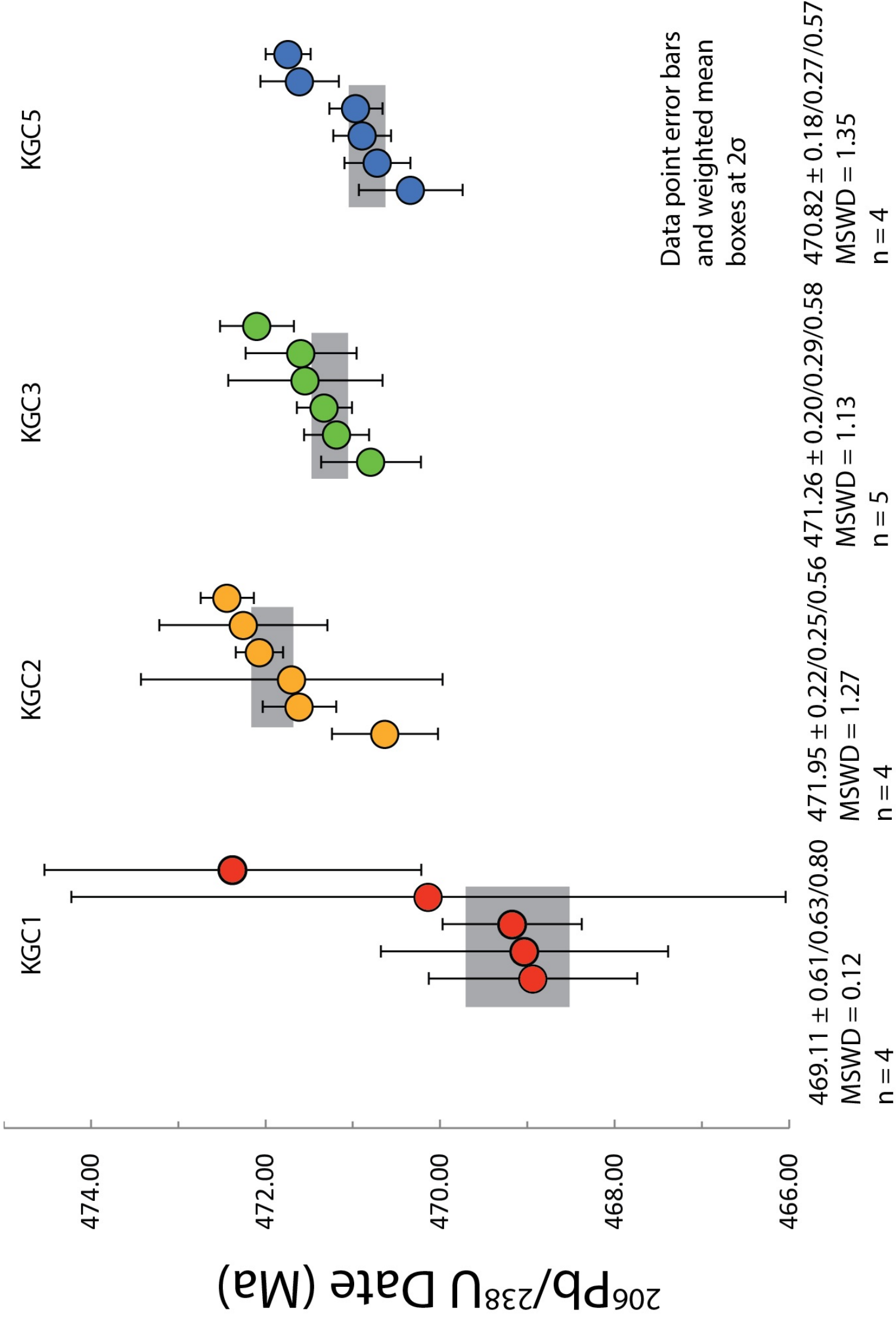


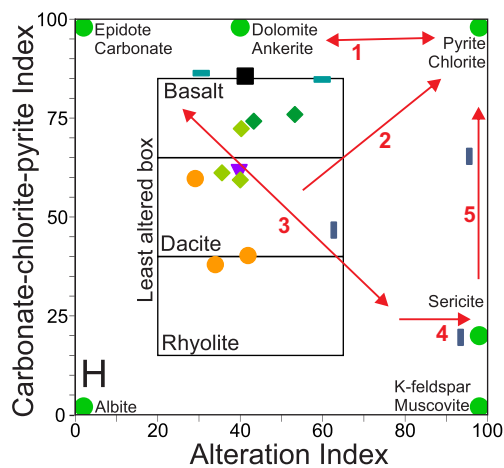
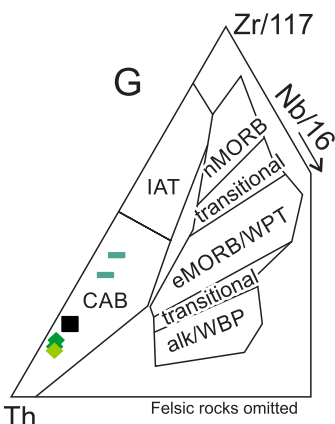
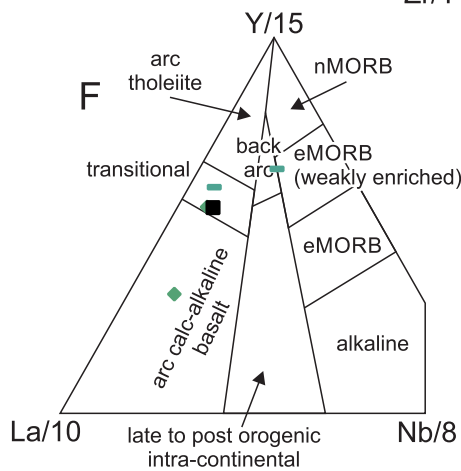
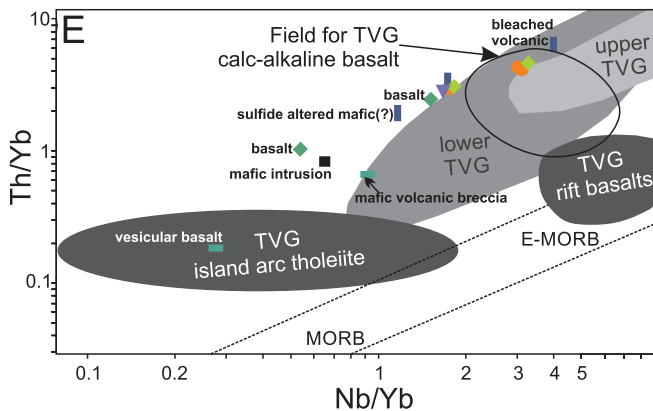
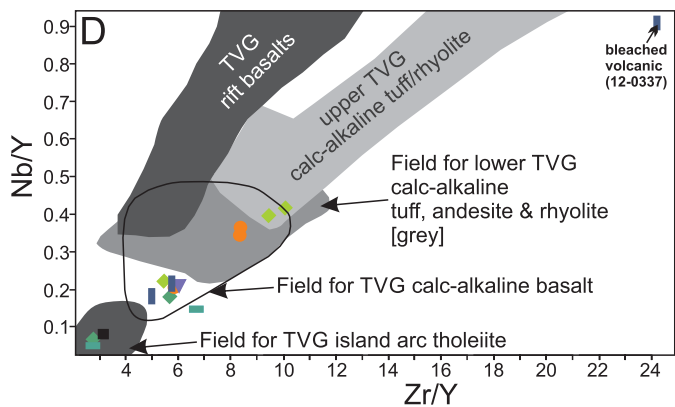
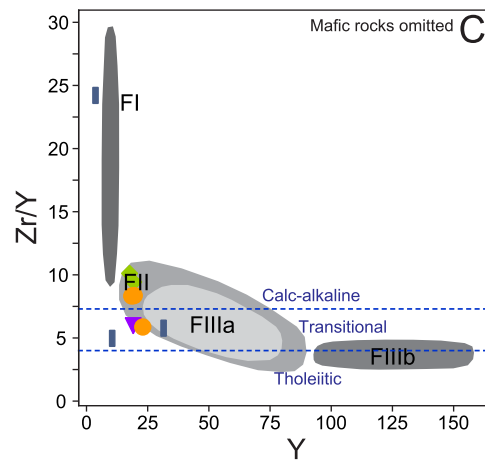
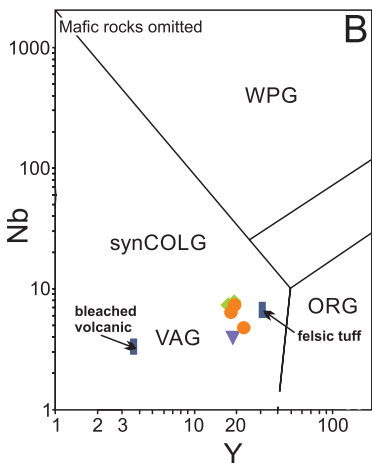
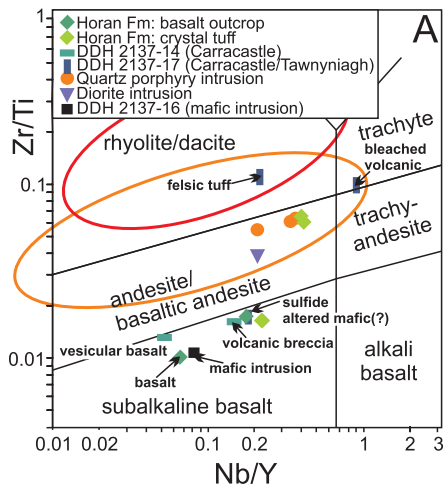
★ Graptolite locality  
 ☆ U-Pb zircon sample  
 ■ Mudstone  
 ■ Tuff  
 ■ Diorite

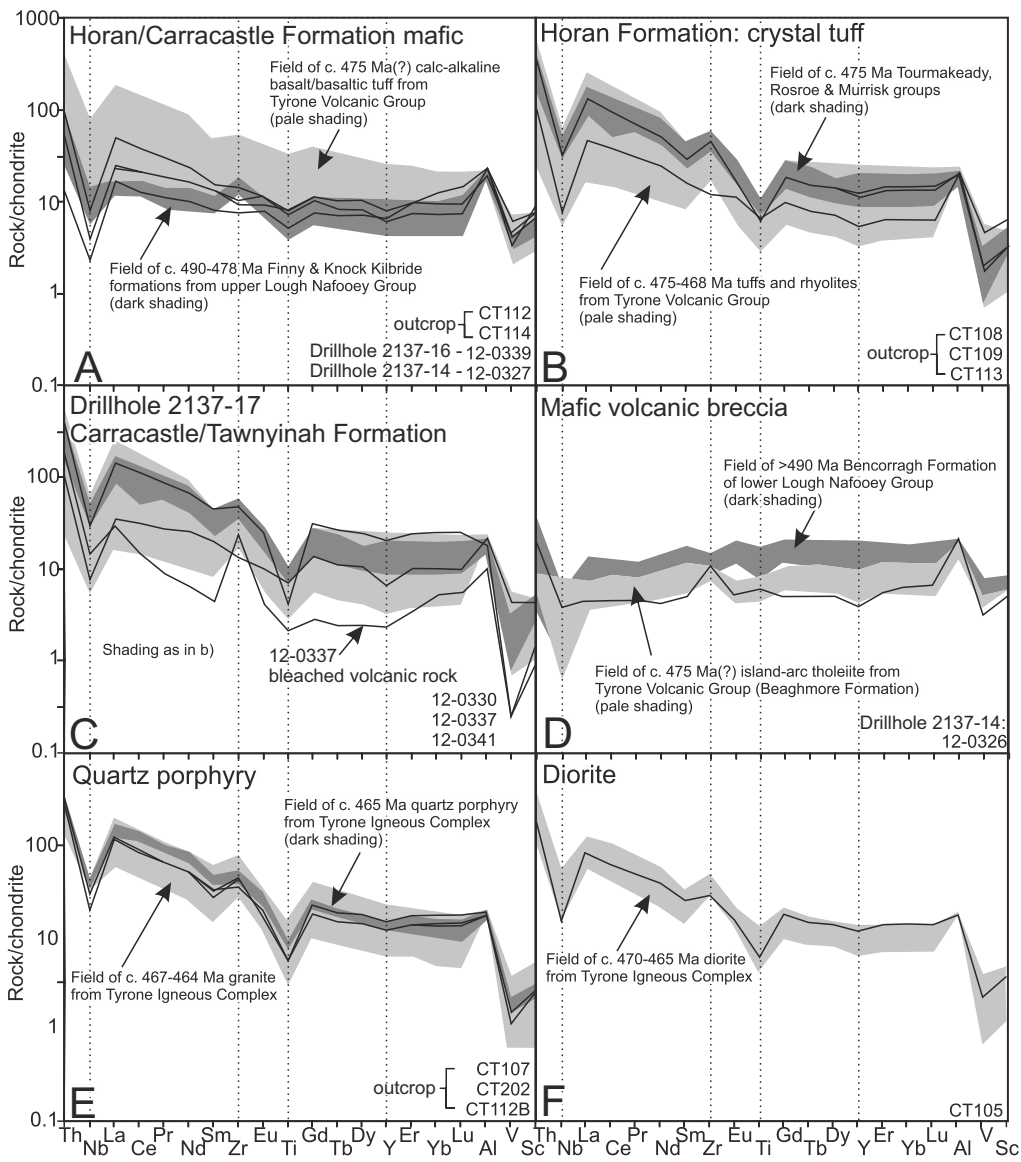


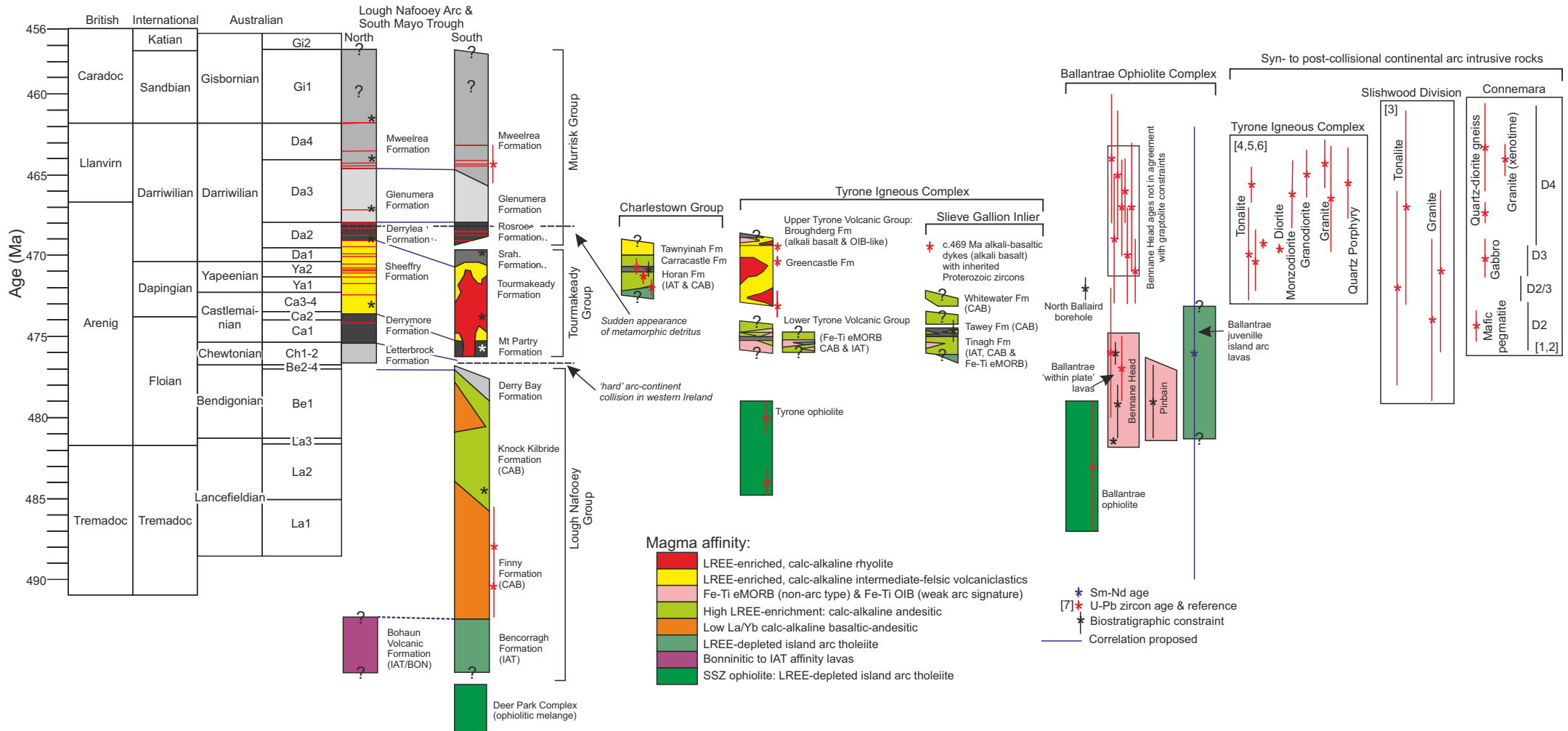


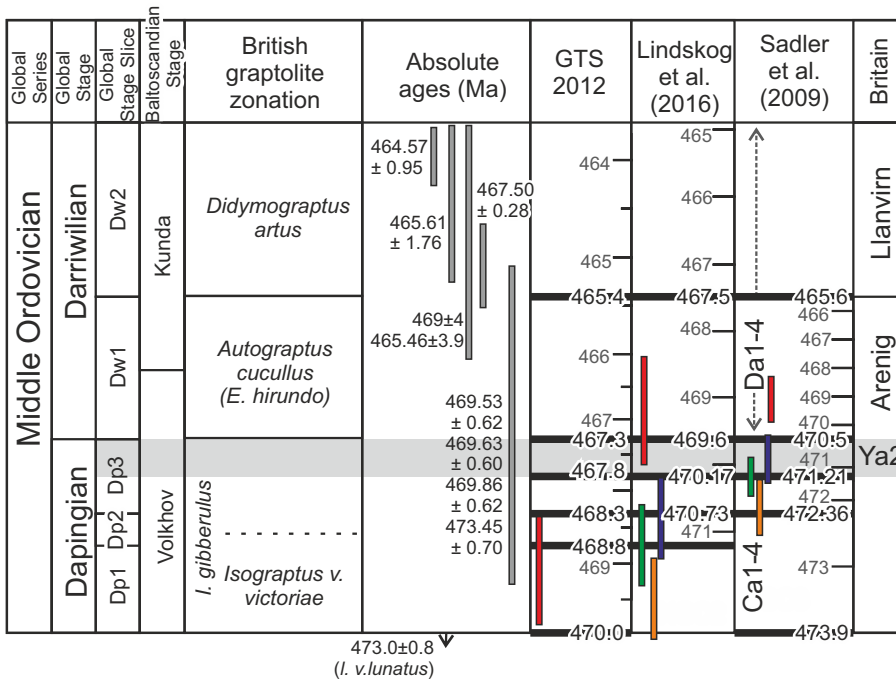












Stratigraphic uncertainty

KGC1  
DIORITE  
KGC2  
TUFF  
KGC3  
QFP  
KGC5  
BRECCIA

473.0 ± 0.8  
(*I. v. lunatus*)

